Bulk defect Passivation: a step towards extended stability of Hybrid Perovskite solar cells

A Thesis

submitted to
Indian Institute of Science Education and Research Pune
in partial fulfillment of the requirements for the
BS-MS Dual Degree Programme

By

Rohitkumar Jadhav

Roll no.20141033

January 2019

Supervisors: Dr.Frédéric SAUVAGE & Dr. Sébastien Gottis

CNRS Researcher
Laboratoire de Réactivité et Chimie des Solides
CNRS UMR7314
Université de Picardie Jules Verne
33 Rue St-Leu
80039 Amiens, Cedex, France

Certificate

This is to certify that this dissertation entitled **"Bulk defect Passivation: a step towards extended stability of Hybrid Perovskite solar cells"** towards the partial fulfilment of the BS-MS dual degree programme at the Indian Institute of Science Education and Research, Pune represents study/work carried out by **Rohitkumar Jadhav** at CNRS Laboratoire de Réactivité et Chimie des Solides under the supervision of **Dr.Frédéric SAUVAGE & Dr. Sébastien Gottis**, CNRS Researcher Laboratoire de Réactivité et Chimie des Solides during the academic year 2018-2019.

Supervisors:

Dr.Frédéric SAUVAGE

Date: 04/11 2019

Dr. Sébastien Gottis

Date: 4/11/2019

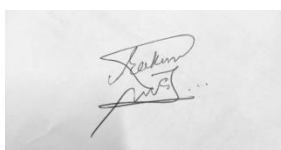Prof. Satish Ogale

Date: 07/11/2019

Rohitkumar Jadhav

Date: 20/10/2019

2

Declaration

I hereby declare that the matter embodied in the report entitled "Bulk defect Passivation: a step towards extended stability of Hybrid Perovskite solar cells" is the results of the work carried out by me at CNRS Laboratoire de Réactivité et Chimie des Solides under the supervision of Dr.Frédéric SAUVAGE & Dr. Sébastien Gottis and the same has not been submitted elsewhere for any other degree.

Rohitkumar Jadhav

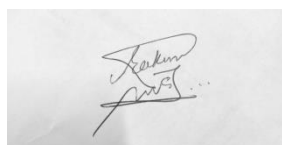Date: 20/10/2019

Dedicated to

Raagya

<u>Acknowledgment</u>

I started my work in perovskites during late 2015 when the field was booming, new and exciting results were coming up every day. I was impressed by the innovative chemistry and fascinating science of these materials. The day to day advances mad eme read the new publications in the field every day. I have always wanted to repay whatever I have received, and by working on solar cell materials, I can deliver excellent results to society. It gives me immense pleasure in presenting my Master's project dissertation entitled, "Bulk defect Passivation: a step towards extended stability of Hybrid Perovskite solar cells." I want to add a few words of appreciation for the people who gave me constant support and guidance throughout my project period.

I have carried out my master's thesis work at CNRS Laboratoire de Réactivité et Chimie des Solides under the supervision of Dr.Frédéric SAUVAGE & Dr. Sébastien Gottis. I want to express my sincere thanks to them for believing in my ability to work in this field and thus, providing me the opportunity to do a Thesis with complete freedom at work: their support, timely suggestion, guidance.

I want to thank my all-time mentors Dr.Satyawan Nagane (Post dot. Cavendish laboratory) and Dr. Aditya Sadhanala (Post doct.Oxford university), who introduced me to this field, the never-ending discussions and lessons have helped me to get a better understanding of these materials. I want to thank my guide Dr. Satish Ogale who gave me the opportunity to work with him for the last three years. He has been very supportive every time. I want to thank Dr. Shreyas Managave, who helped me to connect dots between hybrid perovskites and oxide perovskites formed in the earth's crust. I also want to thank him for supporting my application for this internship.

I want to thank my family and friends for their continuous support, specifically Shubhangi, Devesh, Prayas, Sidharth, Waad, Fionnuala, Iva, Margarita, Ginevra, and Raagya who motivated me in hard times. I'm grateful to have all such lovely people around me.

Rohitkumar Jadhav

Date: 20/10/2019

<u>Abstract</u>

In this thesis, I'm presenting a novel approach to bulk defect passivation. The defect passivation techniques used are usually surface passivating techniques and couldn't stop the self-degradation of the perovskites. The new plan also leads to the formation of new morphologies that are investigated using different characterization techniques. In this thesis, I have tried to compile the recent advancement in passivating methods, their demerits, and merits. Newly obtained morphology in this work could be of interest for the industry, I have also tried to explain how we can move more close to the application of such materials.

Contents

**References**

Chapter 1: Hybrid Perovskite Solar Cells

Energy has been a driving force of human civilizations for millions of years. The requirement of energy has been increasing over these years. As humans have been evolving, the race for survival and a better life, have also been there. The excavation of the natural resources shoots up during industrialization. As a result, we see an increase in the emission of Greenhouse gases in the atmosphere. To fulfill the average energy requirement and keeping the global average temperature almost constant, we should start increasing energy production from renewable sources. The most significant amount of the CO_2 emitting sector has always been power generation. In 2018 global energy demand increased by 4%; as a result, we saw an increase in emission by 2.5% in 2018 and 2.3% in 2017, and the side effects of this increase are evident worldwide.

Photovoltaics has been at the center of Renewable energy generation for the past few decades as the average solar energy received on earth is more than the required power of the Globe. Lower conversion efficiency compared to higher processing cost attributes to the high price per unit of solar energy, which is also the main reason behind the small portion of Renewable energy comes from solar energy. The energy sources like nuclear energy, geothermal energy, wind energy also contribute to the production of Green energy, but solar power has a very less environmental impact compared to other Green energy sources. Direct conversion of solar energy into electricity makes the transportation and storage of solar energy is one more advantage over others.

1.1   Solar cell device

The solar cell is a device which works on the photoelectric principle, the photoactive material absorbs the sunlight and converts it into Electricity. When the photons come in contact with photoactive material and get absorbed, electron-hole pairs are generated, which are collected by the electron transport layer(ETL) and hole transport layer(HTL), respectively, and transported to the connected load.

When an incident photon has more energy to excite electrons into the higher allowed excited state than bandgap energy$(\mathbf{H_g})$, i.e.the forbidden region between lower energy state known as valence band$(\mathbf{H_v})$ and higher energy state known as the conduction band$(\mathbf{H_c})$, then photon gets absorbed by the photoactive material to utilize this energy, the lifetime of the charge carriers in the excited state should be more than the time required by carriers to go into the higher excited states from lower excited states. There are different modes of transitions from $(\mathbf{H_v})$ to $(\mathbf{H_c})$ explained in the below figure.
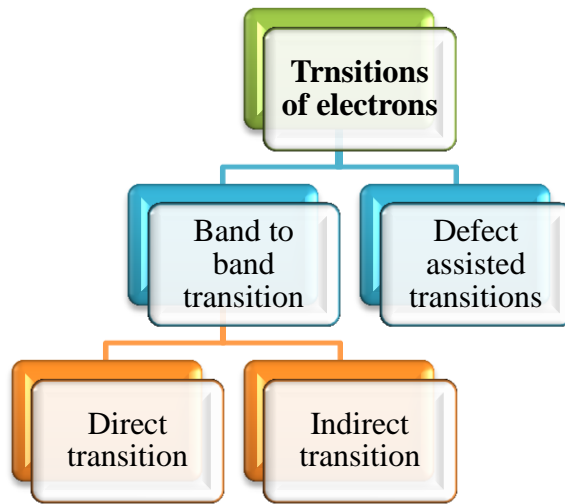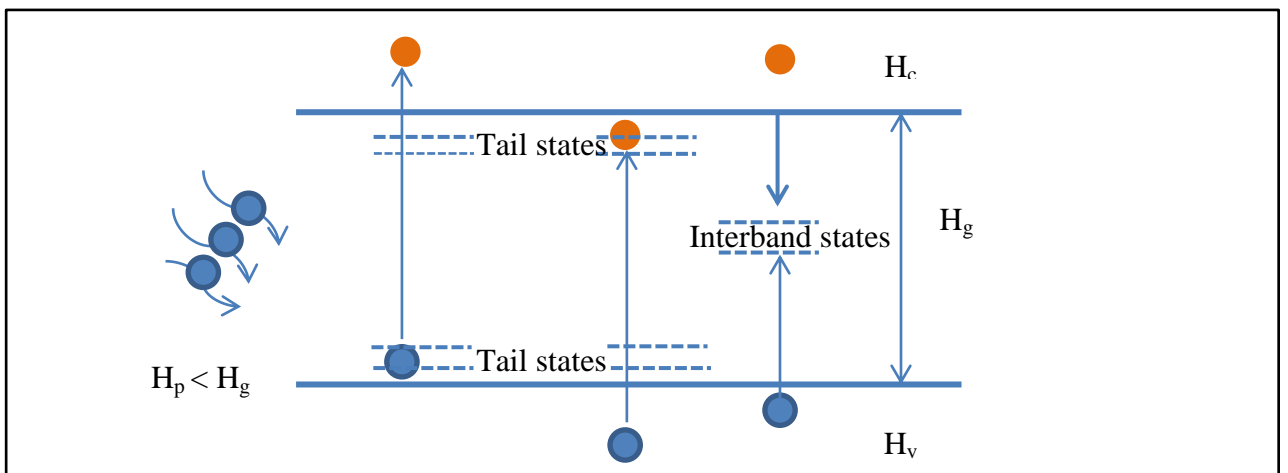
Fig(1.1)

- Band to band transitions-

When a photon of higher energy than the bandgap of the photoactive material is incident, it can go into higher energy levels than the conduction energy before going through relaxation, releasing an excess of energy in the form of heat (hv-H_g).
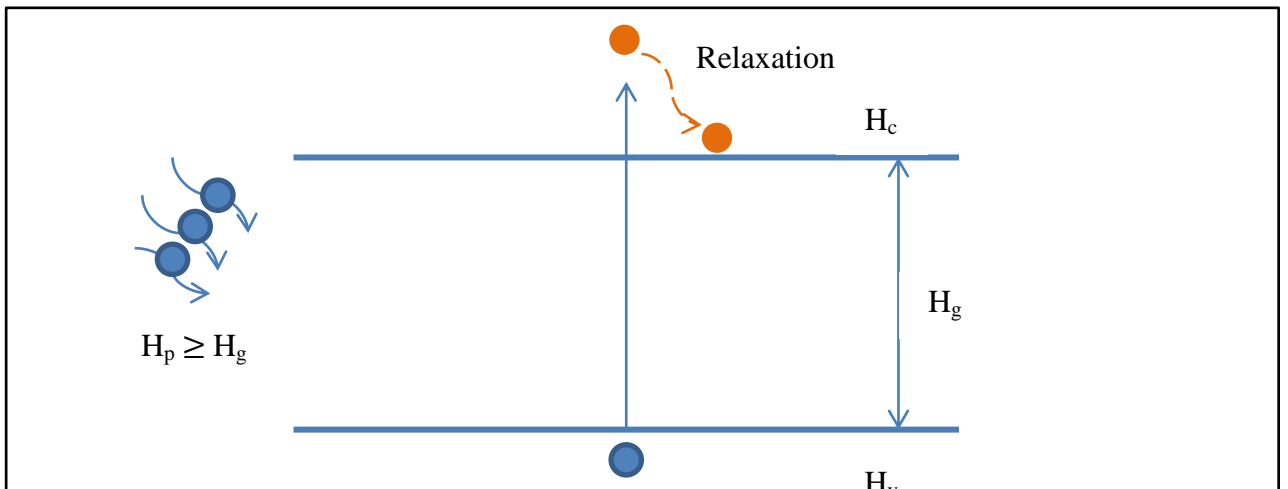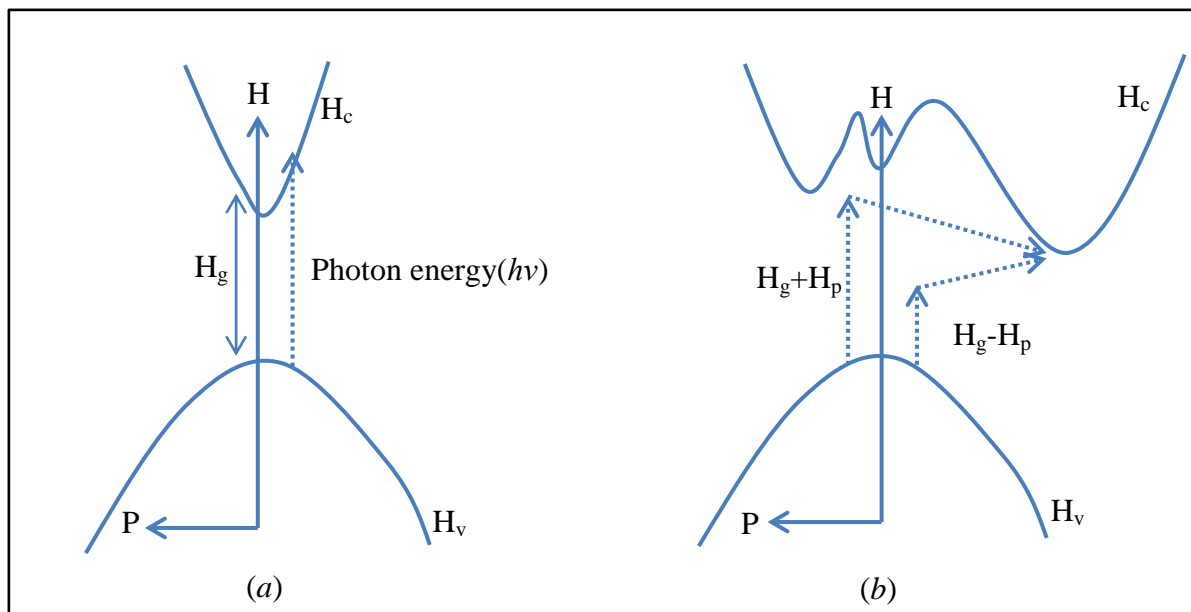

Fig(1.1.a)

- Defect assisted transitions-

Fig(1.1.b)

When the energy of an incident photon is lower than the bandgap of the material, the transition of an electron can occur through tail states, interband states, or both of them. The photon gets transmitted when none of the transitions occur due to the lower energy of the photon.

♦ Direct Band to band transitions-
When there is a change in only energy of an electron transitioning from H_v to H_c as the momentum of electrons and holes in conduction and valence band is equal, then the transition is known as a direct band to band transition. The semiconductors which allow such transitions are known as direct bandgap semiconductors.

Fig(1.1.c)
The absorption of a photon by the band to band transition (a)Direct band to band transition (b)Indirect band to band transition

♦ Indirect band to band transitions-
When there is a change in energy, as well as the momentum of an electron transitioning from Hv to Hc since the momentum of electrons and holes in conduction and valence band, are different, then the transition is known as an indirect band to band transition. The semiconductors which allow such transitions are known as indirect bandgap semiconductors.
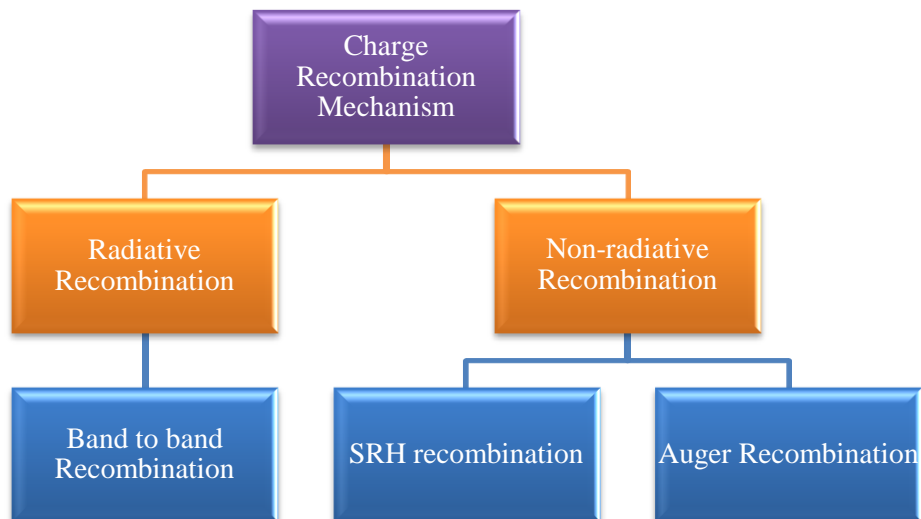
1.2   Charge Recombination

A mechanism of the recombination loses the photogenerated charge carriers. The loss in photogenerated charge carriers leads to the loss in photoconversion efficiency(PCE) of the solar cell. The excited electrons can recombine in two different ways as follows
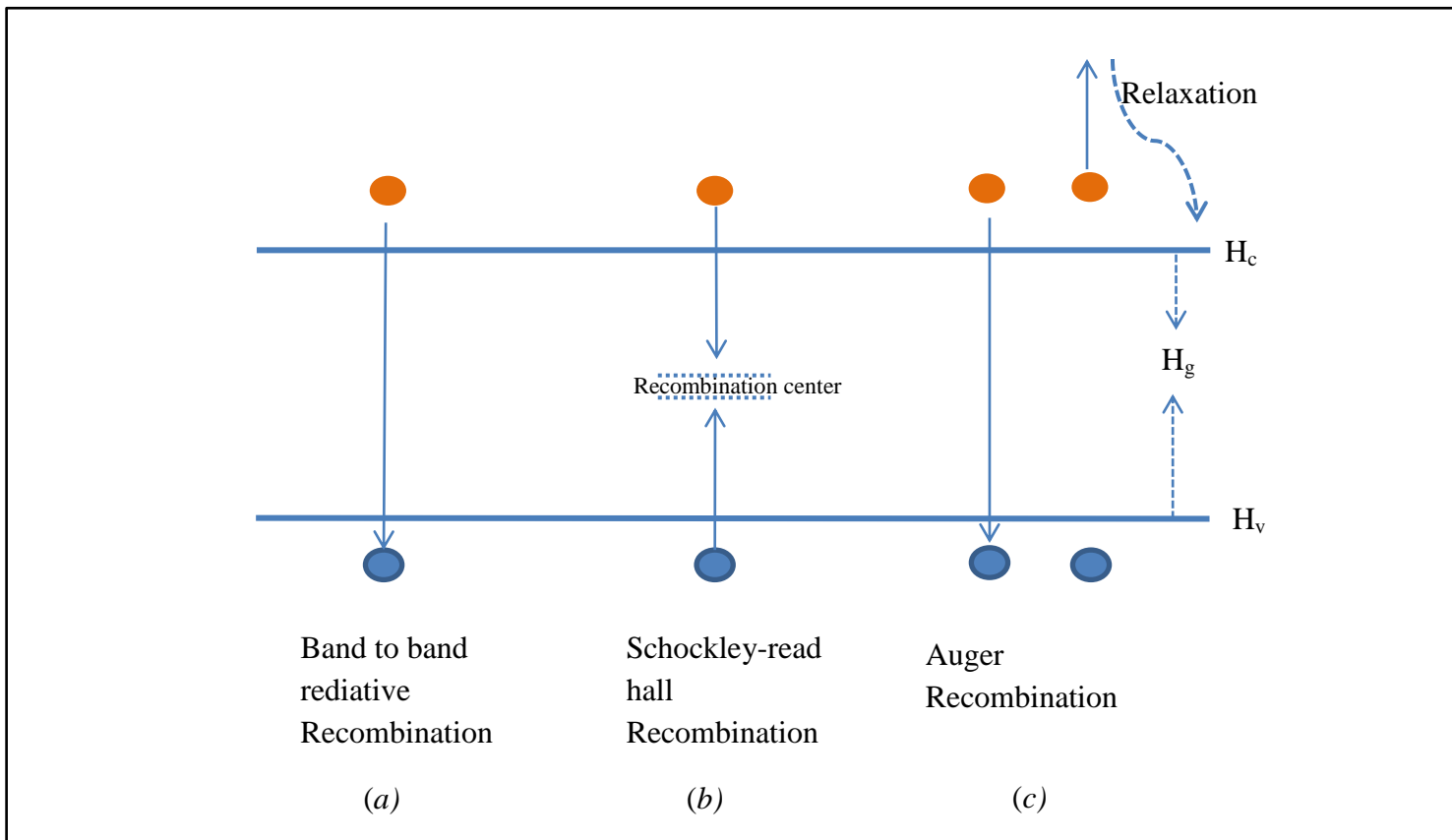

1.2.1 Radiative Recombination

Band to band Recombination [1,2] **-**

When electrons in conduction band recombine with the holes in the valence band of the material they release excess energy in the form of the photon, this liberated energy is equivalent to the bandgap of the material such kind of recombinations are radiative and known as Band to band recombination. The rate of the band to band radiative recombination is given by –

$$R= Q_B(np\text{-}n_i^2) \qquad (1.2.1)$$

Where Q_B is recombination coefficient where n and p are the electrons and holes concentrations, respectively. Whereas n_i is intrinsic charge carriers.

Fig(1.2.1)[1]

Types of recombination mechanisms(a)Band to band radiative recombination(b)Schockley-Read Hall Recombination (c)Auger Recombination

1.2.2 Non-radiative Recombination

Schockley-Read Hall Recombination[1,2] -

When a hole from the valance band and electron from the conduction band recombine at the trap states, which are recombination centers within the bandgap of the material, then the recombination is known as schockley-read hall recombination, or trap assisted recombination. This recombination can take place either inside bulk material or at the interfaces of two different materials. The rate of recombinations of SRH is given by –

$$R=\frac{np-n_i^2}{\tau_p(n+n_1\ )\tau_n\ (p+p_1)} \tag{1.2.2}$$

Where n_1 and p_1 are constants and follows the equations-

$$n_1=n_i e^{\frac{\left(E_{T'}-E_i\right)}{KT}} \tag{1.2.2a}$$

$$\text{and} \quad p_1 = n_i e^{\frac{\left(E_i-E_T'\right)}{KT}} \tag{1.2.2b}$$

$$n_1\, p_{1=}n_i^2$$

the carrier lifetime of electron and holes is given by

$$\tau_p = \frac{1}{C_p N_T} \qquad (1.2.3a)$$

$$\tau_n = \frac{1}{C_n N_T} \qquad (1.2.3b)$$

In the above equations C_p and C_n Are the coefficient of Shockley-Read Hall recombination for holes and electrons respectively. Whereas the N_T indicates the trap state density and lifetime of minority charge carriers is a function of trap state density.

Auger Recombination[1,2] –

When a material is heavily doped, during the process of the band to band recombination or schockley-read hall recombination when the excited electron is in the conduction band. Before going through thermal relaxation, it settles at the bottom of the conduction band. This phenomenon is known as Auger recombination.

The rate of Auger recombinations in n-type semiconductors can be calculated by

$$R = C_A\, n(np - n_i^2) \qquad (1.2.4a)$$

And for p-type semiconductors is calculated by

$$R = C_A\, p(np - n_i^2) \qquad (1.2.4b)$$

C_A corresponds to the Auger recombination coefficient, n and p are electron and hole concentrations and n_i denoting intrinsic charge carriers.

The lifetime of minority charge carriers in Auger recombination is inversely proportional to the square root of the dopant density.

1.3   Perovskite solar cell

In 1954 the first si-semiconductor based p-n junction solar cell reported the record efficiency of 6% at Bell laboratories. The Si semi-conductor based have been dominating the PV market from the last 60 years due to the successful development of both fundamental understanding of physics behind these devices and device engineering. The Si-based solar cell has achieved 26% PCE with an economical fabrication technique before the emergence of the Perovskite solar cells. Over time, there have been other thin-film technologies like CIGS, GaAs, CdTe, which have

shown promising PCE (fig1.3.1)but are expensive for scaling up as a single junction solar cell. GaAs has demonstrated a record efficiency of 29.3% under one sun illumination[3]
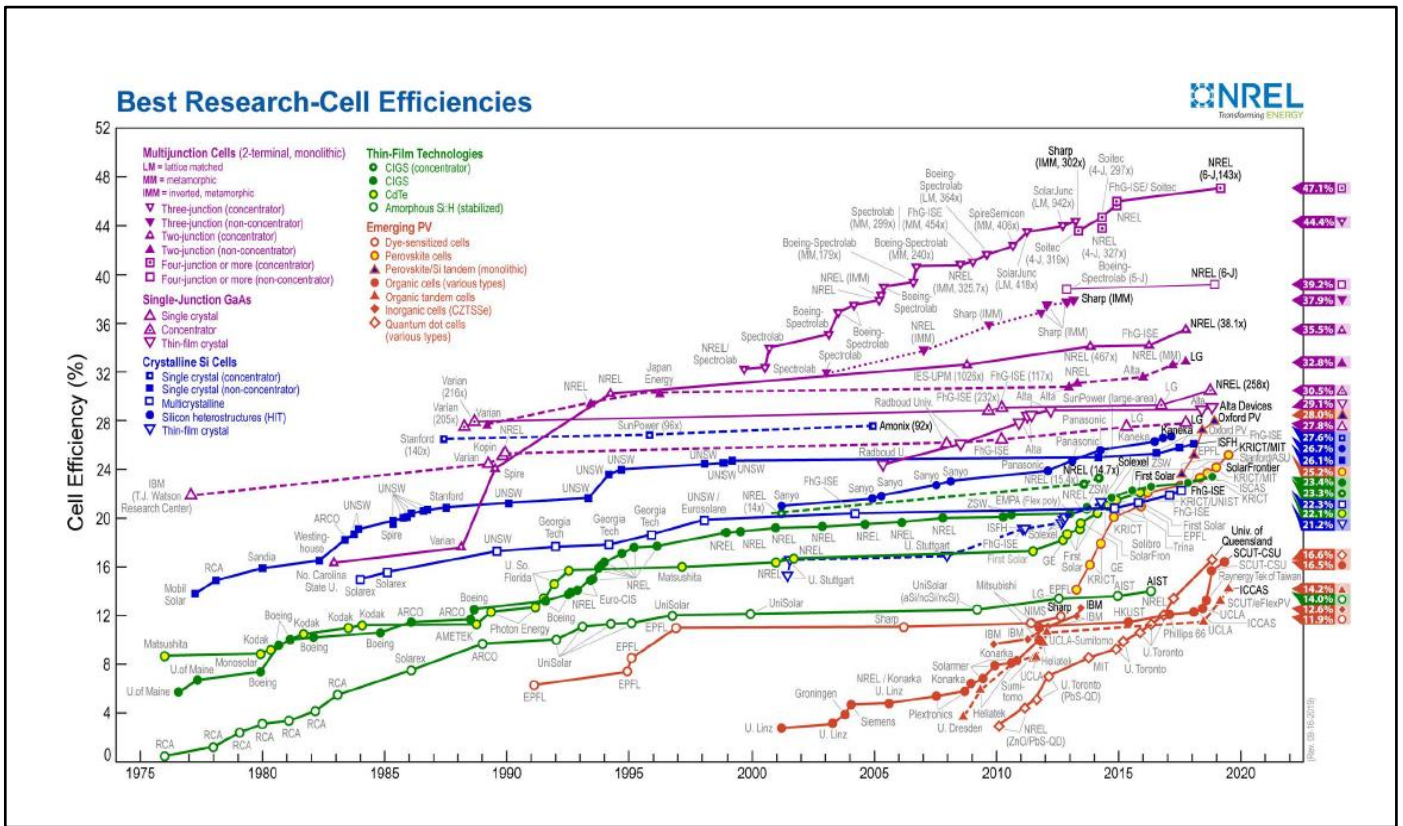
Fig(1.3.1)[4]

NREL efficiency chart updated on August 2019 ("This plot is courtesy of the National Renewable Energy Laboratory, Golden, CO.")

1.3.1 The emergence of Perovskite semiconductors

In 1839 Gustav Rose discovered $CaTiO_3$ the first perovskite material and named it after a mineralogist Lev Perovsky. The compounds having similar crystal structure ABO_3 as $CaTiO_3$ are said to be perovskite structure after the discovery of Goldschmidt in 1926. Perovskites received quick attention because of excellent ferroelectric properties and high dielectric constant of $BaTiO_3$[5]. The perovskites structure can be found not only in oxides but also in halides. Where the halide perovskites are then further divided into hybrid perovskite and inorganic perovskite. Hybrid perovskites contain MA, FA, GA, EA, BA, EA, PEA, Pyr, Cs, Rb, etc. as A-site organic cation, Pb, Sn, Bi, Sb at B-site and I, Cl, Br, BF_4, etc. as anions in ABX_3 Structure. The structure is a cubic structure that has a corner-sharing octahedral network having organic cation at the center of the octahedron.

In the 1950s, Moller observed all inorganic lead halide perovskite with $CsPbI_3$. Later, David Mitzi, in 1998, incorporated organic cation inside the octahedral, which demonstrated excellent electronic properties. The bandgap energies of the perovskite

material reported ranges from (1.1eV) Tin based perovskites to (3.3eV) for chlorine-based perovskite by exchanging A site, B site cations or X side anions.

1.3.2 Advantages over other inorganic semiconductors

It has found that defect tolerance in perovskite is one of the extraordinary properties of this material. The dominant defects in perovskites only create shallow traps, which matches with longer diffusion lengths of carriers and minimum loss in open-circuit voltage. [6] $MAPbI_3$ is a direct bandgap material with 1.6eV optical bandgap, which is less than theoretically calculated bandgap 1.7eV. The absorption coefficient of the perovskite is higher than GaAs, which reduces the depositional thickness of the absorber layer to a few hundreds of nanometer, reducing the processing cost of the solar cell devices. Perovskites possess higher diffusion lengths, which makes them purer semiconductors with excellent charge carrier mobility, due to this extraordinary property, it's easier to incorporate perovskites in planar heterojunction solar cells[7].

1.3.3 Device Architecture

The device fabrication of single-junction solar cells starts with the transparent conducting glass substrate, n-type ETL, Light absorbing perovskite layer, p-type HTL, and back contact. The concept of the mesoscopic Dye-Sensitized Solar cell was introduced into perovskites in 2009 by Miyasaka *et al.* [8] After modifications in the HTL, using different types of mesoporous materials as ETL, passivating layers and various back contact materials the PCE of Perovskites have reached to 25.2% in August 2019. The different device architectures are explained in **fig. (1.3.2)**
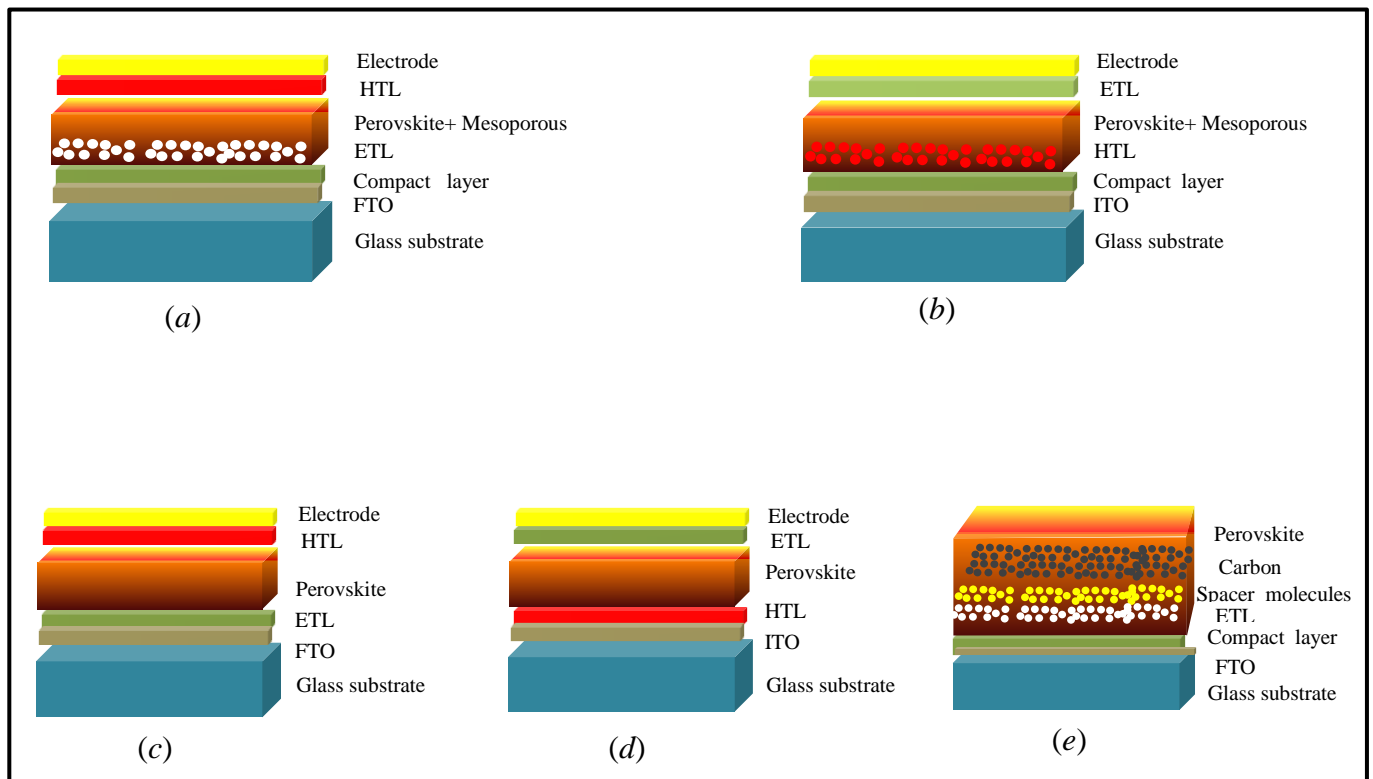
Fig(1.3.2)

Fig(1.3.2) *Different types of device architectures used for stable and efficient solar cell. (a)Standard mesoscopic (b)Inverted mesoscopic (c)standard planar (d)Inverted planar (e)Triple mesoscopic.*

Table 1

Device Architecture	PCE(%)	Efficiency decay	Shelf stability	Testing condition	
FTO/c-TiO$_2$/m-TiO$_2$/Perovskite/ Spiro-MeOTAD/Au	21.6	95	MPP	At 85 °C under full illumination.	[7]
ITO/TiO$_2$-Cl/Perovskite/Spiro-MeOTAD/Au	20.1	90	MPP	500 h under 1-sun illumination without encapsulation and with a 420-nm cut-off UV filter.	[66]
FTO/c-TiO$_2$/m-TiO$_2$/Perovskite/ Spiro-MeOTAD/Au	15.12	87	Shelf stability	In open air with 70% RH for over 500 h without encapsulation.	[69]
FTO/LBSO/MAPbI$_3$/PTAA/Au	21.2	93	Shelf stability	1,000 h of full-sun illumination (including UV radiation, AM 1.5G, 100 mW/cm^2).	[70]
FTO/TiO$_2$/Perovskite/CuSCN/ rGO/Au	20.6	>95	MPP	Aged for 1,000 h under full-light illumination at 60 °C without encapsulation in N$_2$ atmosphere.	[71]
FTO/bl-Cu:NiO$_x$/mp-Cu:NiO$_x$/ MAPbI$_3$/PC$_{61}$BM/bis-C$_{60}$/Ag	18.1	94	Shelf stability	After 1,000 h of dark storage without encapsulation at 25 °C and with <30% RH.	[72]
FTO/C$_{60}$/Perovskite/Spiro-OMeTAD/Au	18.3	80	Shelf stability	After 650 h of aging under full-sun illumination without encapsulation.	[73]
FTO/SnO$_2$/CH$_3$NH$_3$PbI$_3$/RCP/Au	17.3	100	Shelf stability	Over 1,400 h at 75% humidity without encapsulation.	[74]
ITO/c-TiO$_2$/Perovskite/Spiro-MeOTAD/Au	18	60–70	Shelf stability	After 70 d in humidity conditions (from 40% to 50%–70%) without encapsulation.	[75]
ITO/PTAA/Perovskite/C$_{60}$/Cu	20.4	100	MPP	Under 1 Sun equivalent white LED irradiation in a glovebox.	[76]
FTO/NiMgLiO/Perovskite/ PCBM/Ti(Nb)O$_x$/Ag	16.2	>90	Shelf stability	1,000 h in short-circuit conditions to full sunlight.	[77]
ITO/NiO$_x$/Perovskite/ZnO/Al	16.1	90	Shelf stability	Stored in air at room temperature for 60 d.	[79]
FTO/TiO$_2$(perovskite)/ZrO$_2$(perovskite)/Carbon(perovskite)	11.2	100	Shelf stability	Encapsulated, after 10,000 h under 1 sun AM 1.5G conditions at 55 °C and at short-circuit conditions.	[81]
FTO/TiO$_2$(perovskite)/ZrO$_2$(perovskite)/Carbon(perovskite)	10.4	100	Shelf stability	Encapsulated and on the shelf in the dark for over 1 year.	[82]
FTO/TiO$_2$/Sb$_2$S$_3$/CH$_3$NH$_3$PbI$_3$/ CuSCN/Au	5.24	65	Shelf stability	Without encapsulation after 12 h.	[85]
FTO/c-TiO$_2$/m-TiO$_2$/Perovskite/ Spiro-MeOTAD/Au	8.7	>50	Shelf stability	After 12 h of AM 1.5G illumination, using a down-shifting (DS) YVO$_4$:Eu^{3+} nano-phosphor layer.	[86]
FTO/TiO$_2$/CsBr/Perovskite/Spiro-OMeTAD/Au	16.3	>70	Shelf stability	After 20 min of UV irradiation in air without encapsulation.	[89]
ITO/SnO$_2$/Perovskite/EH44/ MoO$_x$/Al	16.62	94	MPP	After 1,000 h of continuous, unencapsulated ambient operation.	[90]
FTO/c-TiO$_2$/m-TiO$_2$/Perovskite/ TTF-1/Ag	11.03	80	Shelf stability	After 360 h in air at a RH of ~40% without encapsulation.	[95]
FTO/TiO$_2$/Perovskite/Al$_2$O$_3$/ HTM/Au	13.07	95	Shelf stability	Under AM 1.5G illumination with encapsulation. for 350 h.	[99]
FTO/TiO$_2$/Perovskite/CuSCN/ Spiro-OMeTAD/Au	12.5	90	MPP	Under AM 1.5G irradiation with encapsulation.	[100]
FTO/TiO$_2$/Perovskite/Spiro-OMeTAD/Cr/Au	20.6	83	MPP	Under 1-sun illumination at 75 °C and a flow of N$_2$.	[103]

16

Above table explains the different materials used in different device architectures, the efficiency after decay and conditions under which the stability was tested.[9](above table is reproduced with the permission from the journal*)

1.4   Aim and Outline of the Thesis

In the past few years,organic-inorganic halide Perovskite has been a promising material for solar cell and LED applications. Despite having excellent photoconversion efficiencies(PCE) and intermediate bandgap, this material has been struggling with temperature, moisture, oxygen, and photoinduced instabilities. In this study, we will discuss the degradation mechanism of photovoltaic Perovskite material, how shallow traps, deep traps, surface defects, grain boundaries, and grain size affect the PCE, FF(fill factor), Voc(open circuit voltage) and Jsc (short circuit voltage) towards the end of the thesis.

In **chapter 1,** I have discussed solar cell devices, the evolution of the perovskite solar cell, different recombination pathways, and various device architectures.we also discussed remarkable properties of perovskite solar cells.

In **chapter 2,** I will discuss the degradation pathways, which cause a loss in PCE of the perovskite solar cell, after understanding the degradation mechanism, I will discuss previously used defect passivation techniques and their flaws according to me. I introduce a new method of deep trap passivation through the molecular vapors towards the end of this chapter and conclude the section with the experimental setup.

In **chapter 3,** I present the results obtained from different characterization techniques and their significance.

In **chapter 4,** I will first build up a theoretical approach to explain the obtained results, which will be an extension of chapter 3, conclusion, and future perspective of the idea.

Chapter 2: Iodine a Curse, or Boon?

It is believed that the defects in different layers of the HPVSC(Hybrid perovskite solar cell) device can affect PCE, FF, Voc, and Jsc during the operation of the device. Under illumination, electrons from the valance band are excited into the conduction band, which further splits quasi-Fermi levels of electrons and holes. The splitting is maintained by Free charge density at which the rate of charge recombination and the rate of charge generation are equal. The quasi-Fermi level splitting of electron-hole pair generates potential known as Voc. Nonradiative losses decrease the steady-state free charge density, which reduces the Voc of the HPVSC device. Shockley Read Hall is the process by which non-radiative loses occur due to the trapping effect of deep level traps. Passivation of such traps can be done to enhance the FF and Jsc of the HPVSC devices. Deep level traps and Auger recombination are the dominant processes of non-radiative recombination of charges in semiconductors. Eli *et al.* have recently proved that Auger recombinations are relatively less in HPVSC under solar illumination. [10] When deep level traps are created by defects, the nonradiative recombination occurs through Shockley-Read- Hall process.2 It is necessary to reduce such defects to enhance the PCE and stability of HPVSC. [11] Researchers have come up with exciting solutions to overcome such defects by following methods-

1. Surface passivation.
2. Incorporation of layered or 2-D materials as spacers in Bulk perovskite layer(thickness 300nm-400nm).
3. Doping of HTL/ETL
4. Metal alloying.
5. Mixed halide perovskites.

Techniques mentioned above shown better Performance, but the maximum PCE didn't stay constant for a longer duration, which is approximately 25 years in the case of Silicon solar cells. The main reason behind the degradation of these materials is Free I- ions present in the perovskite layer. The passivation of surface or doping of the hole transport layer(HTL) can stop migration towards metal contact, but it can not prevent the self-destructive nature of the undercoordinated Iodine molecules. In this work, we will study the degradation of the perovskite in different conditions; we will try to passivate iodide defects by I_2 vapor exposure and how it affects the radiative and nonradiative losses. In the latter part of the work, we will use some Fluorinated organic spacers, which can bond to under coordinated iodine ions and reduce the degradation of the Perovskite layer.
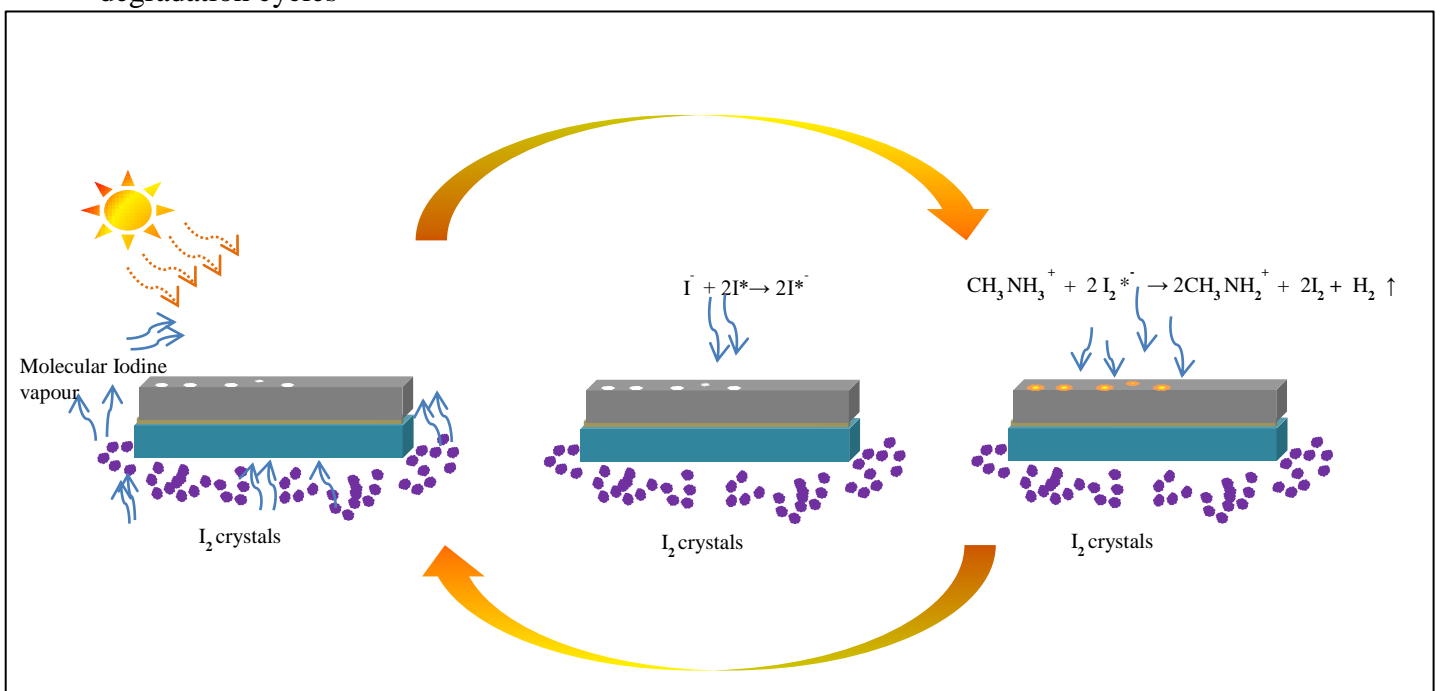
2.1   Degradation of Perovskites

In 2015 Yabing Qi *et al.* investigated the effect of the Iodine in catalyzing the water

and oxygen assisted degradation of the perovskites. [12] In this work, they prepared the MAPbI$_3$ perovskite devices with the Ag electrode, which further placed in different conditions to study the degradation in detail.

The different set of samples had -:

1)Glass/FTO/TiO$_2$/Perovskite/spiro

2) Glass/FTO/TiO$_2$/Perovskite/spiro/Ag

They kept both of the above devices in ambient conditions and Inert atmosphere. They observed corrosion of the Ag top electrode and formation of AgI, concluded from XRD and HRXPS. The interesting part of this work was the formation of AgI in devices kept in an inert atmosphere.based on the results team proposed degradation mechanism of the perovskite in the presence of the Moisture and Oxygen. When hole-transporting material is spin-coated on the perovskite layer, the HTM has already developed pinholes. When these films come in contact with moisture and oxygen, the MAPbI$_3$ breaks down into HI and MAI, leaving PbI$_2$ on the substrate, which further collapses the structure of the perovskite and degrades it. To get more insights from the mechanism of degradation, the team took this work to the next stage, where they studied the effect of molecular iodine on perovskite thin-films. The exposure of the molecular iodine leads to the formation of I* ions in the perovskite under the illumination of UV- light. These I* ions react with undercoordinated Iodine ions to form I$_3^-$, which reacts with Methyl ammonium ions to undergo formation of HI, MAI, and more I molecular iodine, a crucial reason of degradation cycle. The figure below explains the degradation cycles-

Fig(2.1.1)

The fig(2.1) shows cyclic degradation of the halide perovskites by I_2 vapor under the illumination of the UV- light, when the similar films kept in the dark the formation of lead iodide was observed again, and the mechanism can be explained by the fig(2.1.2)
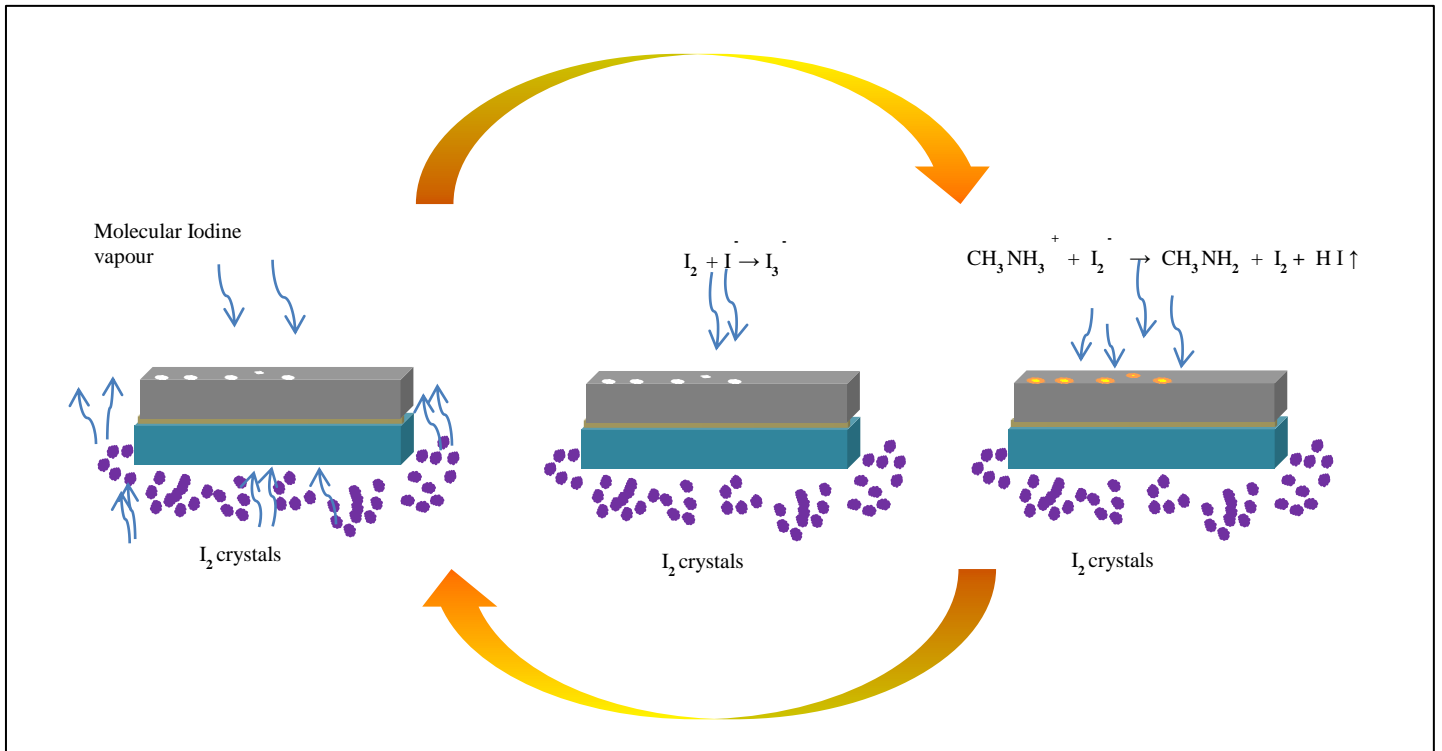
Fig(2.1.2)

They concluded that the PbI_2 formation is independent of the conditions in which films are kept. If the perovskite layer has an excess of undercoordinated Iodine ions, it'll be enough to start cyclic degradation of the perovskites. In the next section, I'll discuss different passivation techniques and their working principle.

2.2   Surface Defect passivation

The defect passivation technique came in the picture when it was observed that the pinholes in the HTL are leading towards the leaking of the metallic top electrode into the perovskite layer, causing a drop in open-circuit voltage and some times shorting of the solar cell devices. It has been found that the ionic nature of HPV brings an imbalance of charges and creates either positively or negatively charged defects. These defects could be passivated by materials which form ionic or coordination bond with these defects. To form coordination bonds with these defects, because of their positive as well as negatively charged nature. the defect passivation techniques can be classified depending upon nature of bond formed

between defect and passivating material as follows **-**
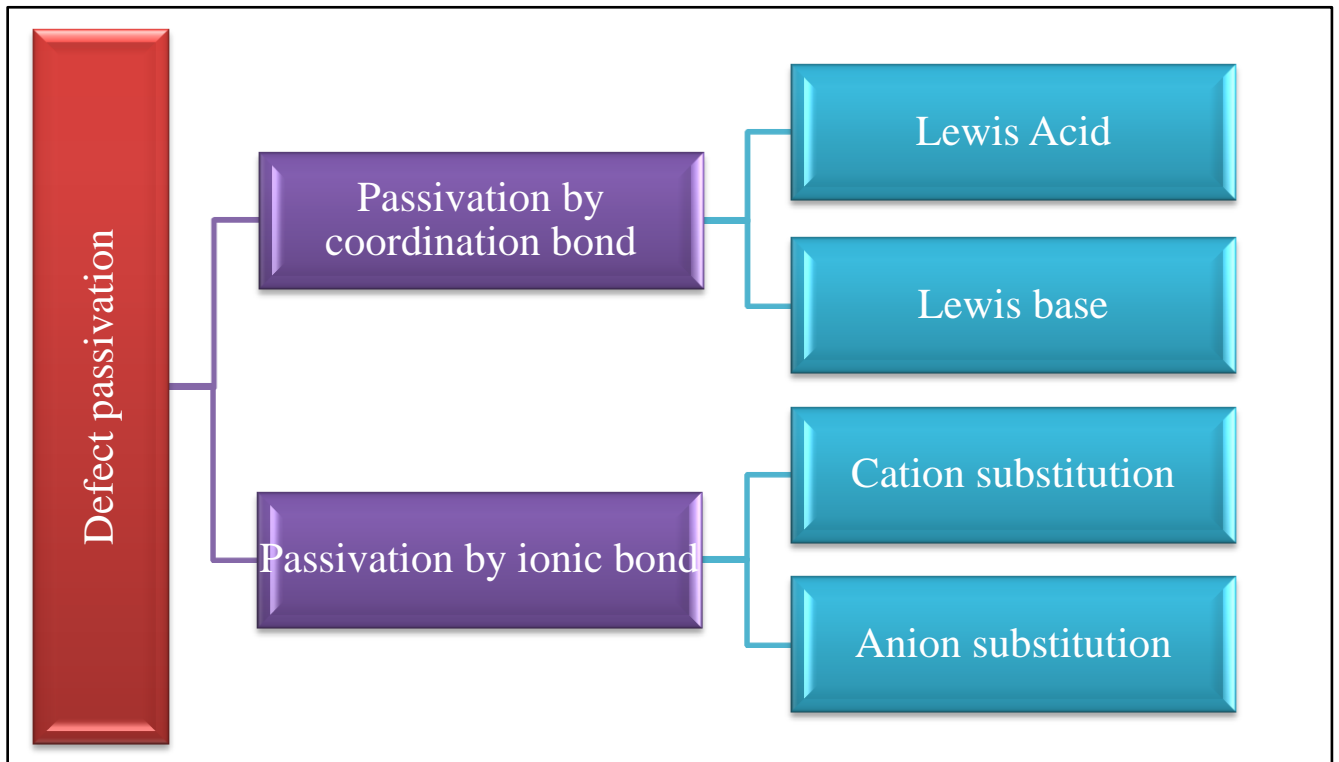
Fig(2.2)

2.2.1   Passivation by coordination bond

Lewis Acid- C60 and it's other derivatives like (PCBM/ICBA) have shown enhancement in the PCE of the HPVSC[14,15], The C60 forms coordination bond with undercoordinated PbI3-. The bond forms because of the strain induced by C60 and not because of chemical reactivity. The stability of the devices enhanced after the addition of Lewis acid, but still, it's not comparable to the silicon solar cells.

Lewis Base – The addition of Lewis bases can form bonds with undercoordinated Pb^{+2} and clusters formed because of lead by sharing nonbonding electrons. It has been observed that passivation by Lewis bases has to lead to a decrease in non-radiative losses by developing Lewis adduct.[16,17]

2.2.2   Passivation by ionic bond

The ionic bond passivation technique depends upon the nature of the defect. The passivation could be done by either Cation or anion. This passivation technique involves complete sharing of electron or proton to allow electrostatic interactions.

Addition Of Cations- Metallic cations like Cs and Rb, organic cations like Formamidinium, Guanidinium have been extensively used to passivate

undercoordinated PbI3- defects and Methylammonium vacancies. The addition of the metal ions in the bulk perovskite layer can stop the formation of Frankel defects by occupying interstitial sites. The direct evidence of these cations going into grain boundaries and perovskite lattice yet to come. Besides metal cations, researchers have used organic cations like Butylammonium, Octylammonium, Phenylethylammonium, and diammonium derivatives.

Addition of Anions- Passivation by addition anions have not explored much. There are very few reports of passivation by Cl^- in the form of MACl, CsCl, FACl. The reason behind not using anions for passivation is an addition of anions like Cl^- and Br^- increases the bandgap of the perovskite and will decrease the PCE.also addition of different halides with iodine leads to ion migration and phase segregation which ultimately results in decreased PCE under solar illumination. We have reported a novel material that shares BF^- anion. The addition of BF_4^- slightly changes the bandgap by a few electron volts and brings the photostability to the perovskite layer.

2.3 Bulk defect passivation-

In the first section of this chapter, we discussed the degradation mechanism of perovskites caused by undercoordinated iodine ions. In the second section, we discussed how researchers have come up with different passivation techniques to tackle the long term stability and high PCE over time. The fig. (2.3.1) explains the various defects that can form inside the hybrid perovskite structure and the binding sites of the passivating materials.
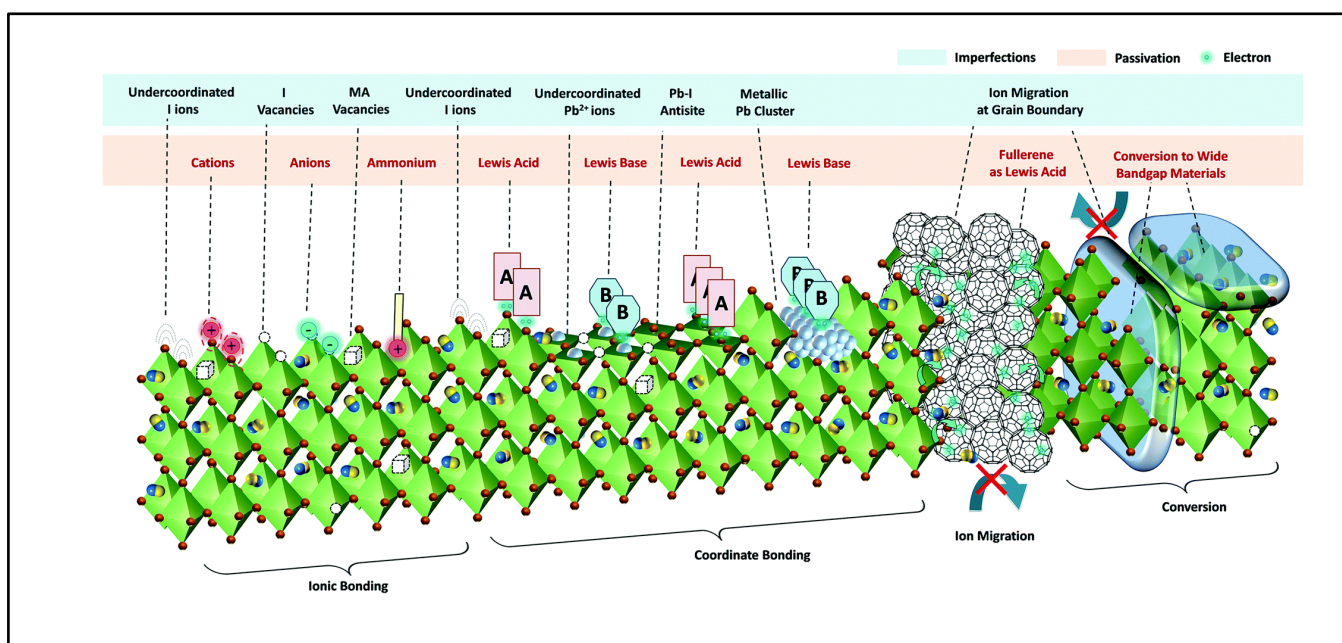
Fig(2.3.1)

*Imperfections in HPV film and their passivation by ionic bonding, coordinate bonding, and conversion to wide bandgap materials, and suppression of ion migration at extended defects.***(The above schematic is reproduced with permission from the Journal RSC).**[18]

2.3.1 Flaws in existing passivation techniques

The origin of different defects could be mixed and could contribute towards shallow as well as deep traps, which can lead to radiative and non-radiative losses, respectively. Sargent *et al.* showed in their work on the mismatch of the cations and anions in perovskites, which can lead towards the different shallow and deep traps depending upon the nature of the defect. [19] The **fig. (2.3.2)** explains how different halide can contribute to various defects in perovskites. The passivation techniques used so far have succeeded in decreasing the migration of free ions towards the electrode, which eventually reduced the hysteresis and improved the stability in the output of PCE, but the stable output didn't stay for a longer duration.

The main reason, according to me, behind loss in PCE over time is good evidence of the degradation of the material. Most of the passivation techniques stop the diffusion of ions, but they aren't able to stop the self-degradation mechanism since those are surface passivation techniques. Even if the perovskite surface is smooth and compact, the undercoordinated ions can start the degradation cycles within the bulk perovskite layer.

2.3.2 Effective Passivation approach

I introduce an idea of bulk defect passivation in this work, which can stop the undercoordinated ions from starting the degradation cycle. I have focused on the passivation of undercoordinated iodine ions because of the volatile nature of the Iodine in the presence of light, moisture, and oxygen. In this work, I planned to passivate the Iodine defects by exposing the spin-coated thin-film of the perovskite layer to Molecular iodine vapors during the formation of the perovskite phase of the material. After annealing of the films, we plan to treat it with iodopentaflurobenzene, which can bind to excess for iodine to stop the reverse effect of the iodine. The details of the experiment are discussed in the next section of this chapter in detail.

There have already been some attempts to passivate the iodine defects. Sang Seok *et al.* published a work where they included the molecular iodine in the precursor solution of formamidinium lead halide perovskite and got more than 21% PCE and 500 hours of stability. [20] Even though these devices had high PCE, but Stability of the device was not comparable to other reports. The reason behind the less stability could be excess of Iodine in the bulk layer. Because of this reason, it's crucial to treat I_2 treated films with Iodopentaflurobenzene, which can bind to these undercoordinated iodine ions and stop them from migrating. The way to confirm that iodide defects have been passivation can be concluded from the longer decay time of the charge carriers, compact morphologies of the thin film devices with fewer grain boundaries, and bigger defect-free crystals.
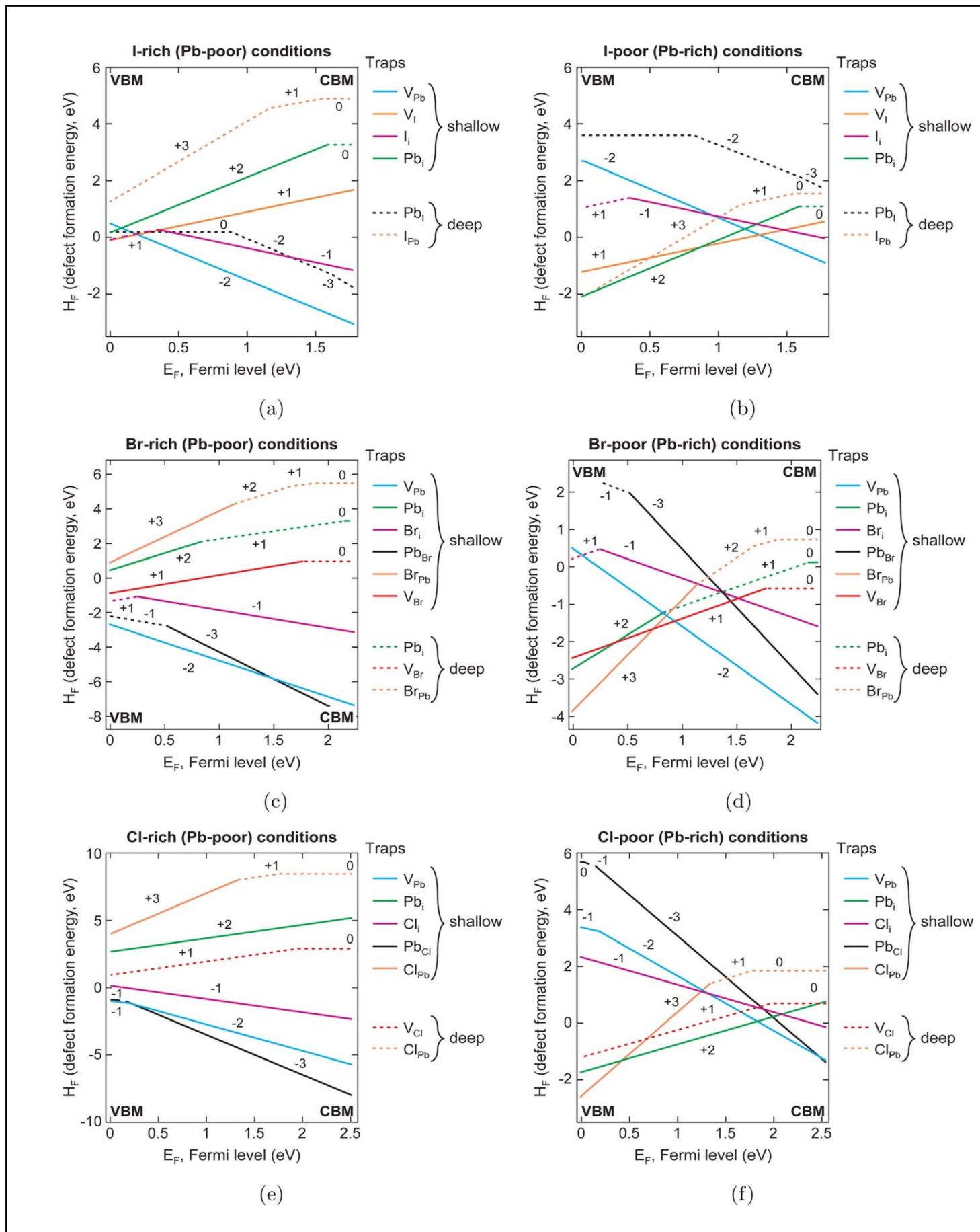
Fig(2.3.2)

2.4 Experimental Insights

2.4.1 Experimental method

The volatile nature of Iodine, especially vapor makes it more vulnerable to handle the inside glovebox. To deal with this problem, I spin-coated MAPbI$_3$ perovskite on FTO coated glass substrates. An airtight jar with 1 gm of iodine crystals is already put into the glovebox, the spin-coated film then was transferred into the jar. Then the jar was put into the oven for annealing of thin-film and evaporation of iodine crystals simultaneously. After the different times of exposures, the thin-films are transferred back into the glovebox for further annealing for 30 minutes. The schematic in **fig.2.4.1** shows the sample preparation method.
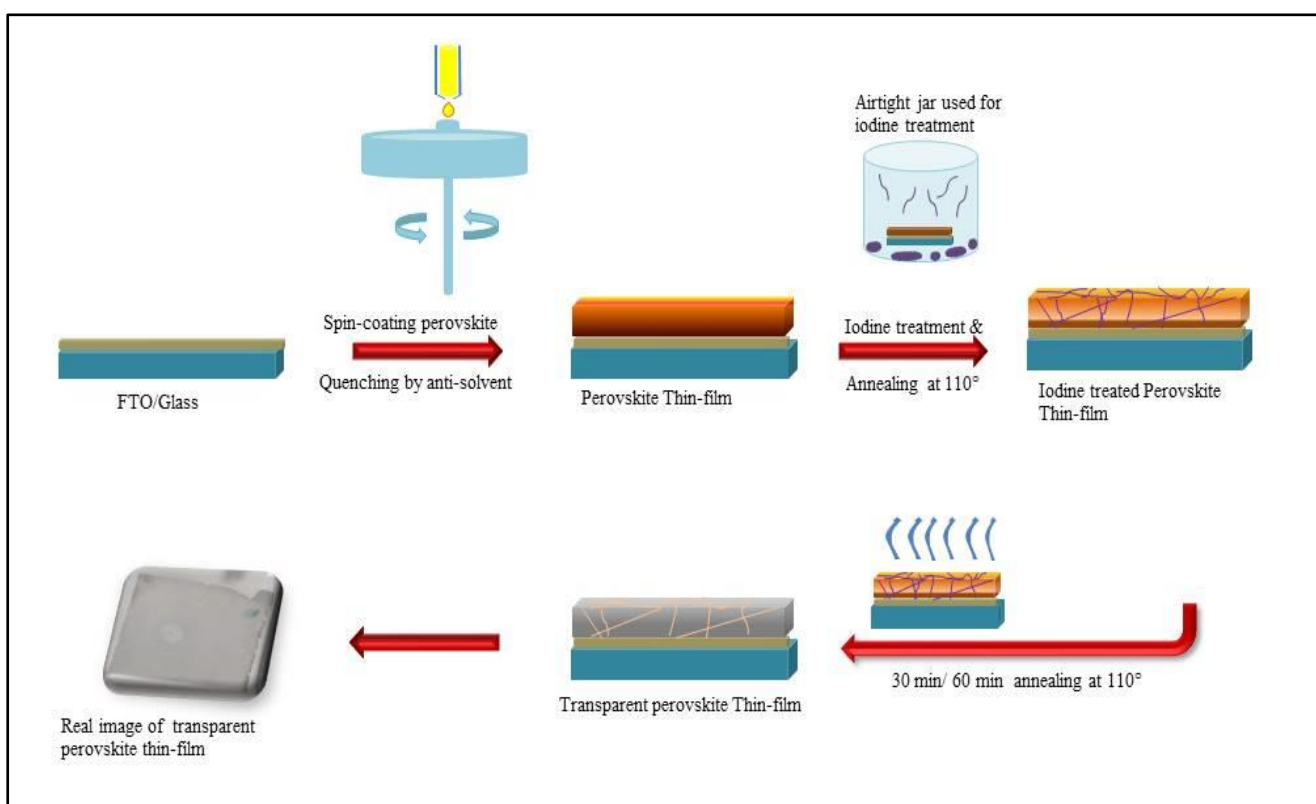
Fig(2.3.2)

One of the exciting findings of the above experiment was to see a reasonably transparent thin-film which wasn't expected. I will discuss these transparent thin-films in the next section of this chapter with results from different characterization techniques and their analysis.

2.4.2 Sample preparation

Thin-film

In the first half experiment was performed with $MAPbI_3$ perovskite. For these films, the precursor salts, MAI, and PbI_2 taken in 1:1 molar concentration in vail. Then the precursors are dissolved in 80%:20% DMF, DMSO respectively in volume percent of total 1 ml. The main reason behind adding DMSO is to slow down the crystallization and form uniform grain size and compact thin-films.

To quench the films around 200ul of Toluene was used at the last 10 seconds of the spin-coating. For making ideal films, different annealing method was used to confirm if the results are independent of the annealing technique, keeping time constant. We perform Post-treatment Annealing in Oxygen atmosphere, which leads to the formation of Cs_2O in the case of $(FA_{0.83}MA_{0.17})_{0.95}Cs_{0.05}(PbI0_{.83}Br_{0.17})_3$, i.e., triple cation perovskite. To avoid the formation of Cs_2O, after treatment, the jar is transferred into the glovebox for annealing on the hot plate in the Argon atmosphere.

Solar cell device

FTO substrates are cleaned first using soap solution and then ethanol. Cleaned substrates then itched after taping with 1M HCL and Zinc dust. After itching substrates are cleaned again to confirm no impurities on the surface, then the substrates were heated to 200°C for 20 minutes to evaporate any organic impurity and transferred into the UV-Ozone chamber for final cleaning. The cleaned substrates then spin-coated with 1M TiO_2 solution and put for stepwise annealing for 3 hours. To get rid of the remaining pinholes, 0.5M TiO_2 solution was spin-coated and again annealed. The films then spin-coated with mesoporous TiO_2 solution prepared by dissolving TiO_2 paste in butanol and annealed. The 300 n.m. thick layer of $(FA_{0.83}MA_{0.17})_{0.95}Cs_{0.05}(PbI0_{.83}Br_{0.17})_3$ was spin-coated and quenched by 400ul of Chlorobenzene. The rough morphology of thin-film confirms the uniform size of grains. Spiro-OMeTed doped with LiTFSI in 1ml chlorobenzene was spin-coated on top of the perovskite layer. In the end, 80n.m. of the Au electrode is thermally deposited. Silver paste is coated on top of electrodes to avoid scratching by crocodile pins.

2.4.3 Characterization techniques

X-ray diffraction

All X-ray diffraction experiment has been performed on D8 copper by Bruker. We mounted thin-film samples on the standard sample holder. The setup arrangement is explained in the fig. (2.3.3)
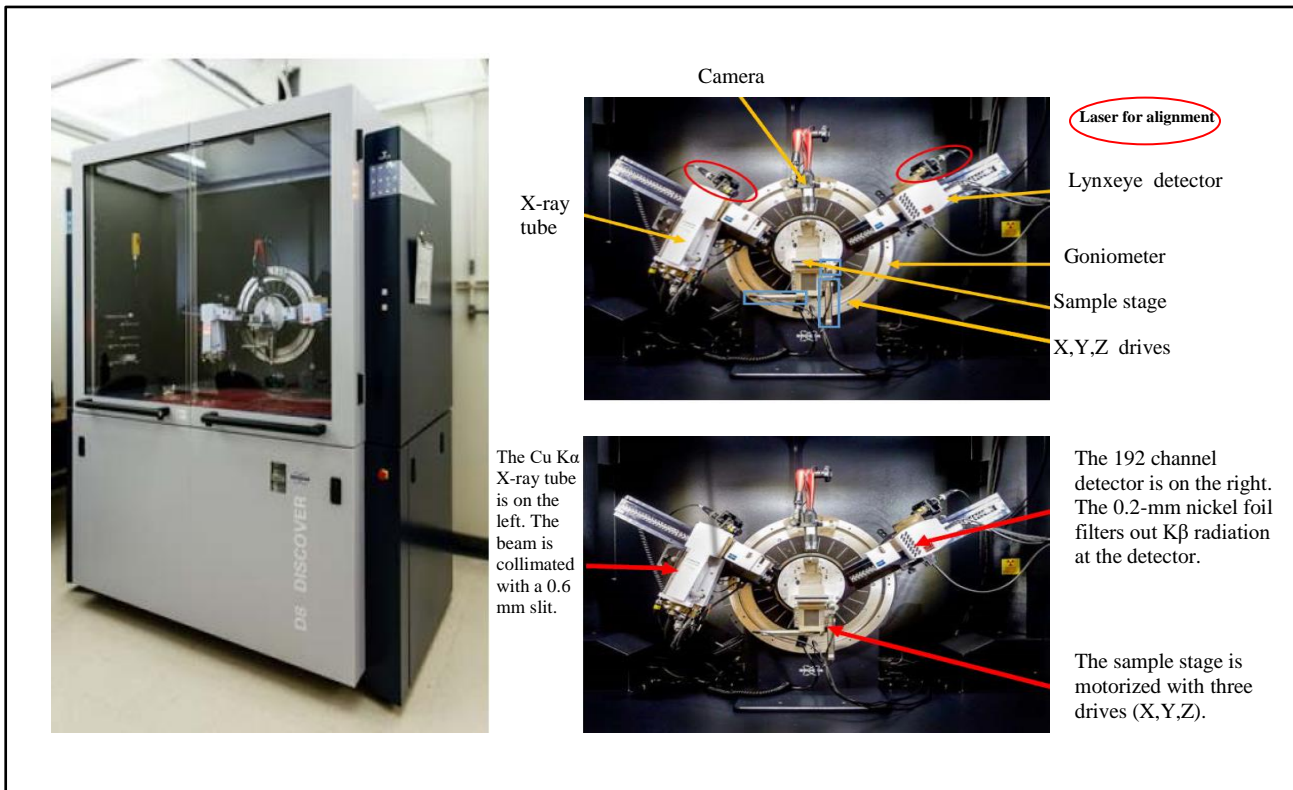
Fig(2.3.3)

Steady-state Photoluminescence & Tcspc

FLS-980 from Edinburgh Instruments was used to perform Steady-state photoluminescence measurement. The setup has a 450 W Ozone free Xenon arc lamp with a detection limit from 230nm – 850nm with a PMT detector. The excitation wavelength used for the samples was 475n.m.
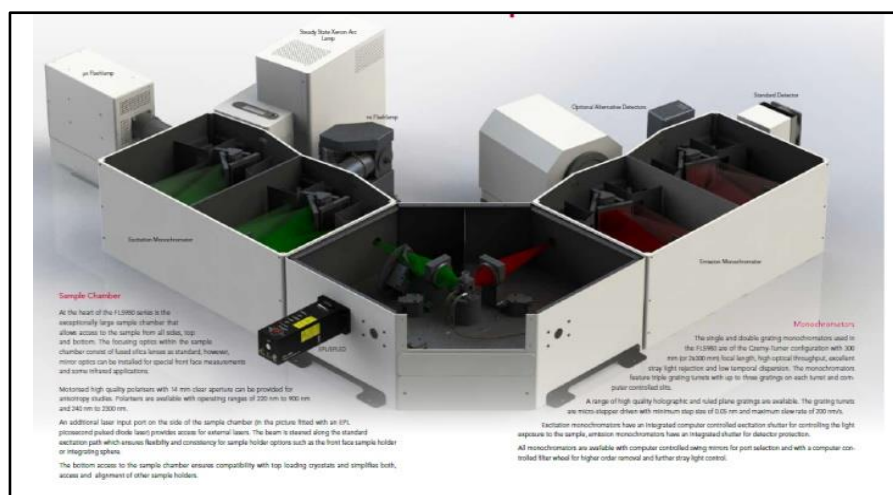
Fig(2.3.4)

The TCSPC measurements are have performed on the Thin-films of perovskites using the same setup with the 475nm Laser and PMT detector.

UV-Vis absorption

Carry 5000 is used to calculate the transmittance of the thin-films in this work. The integrating sphere is used to measure the transmittance of the thin-films, with a deuterium lamp as a source. The results obtained from the spectrometer are analyzed by Carry software package.

SEM Imaging and EDX

Imaging and the analysis of the thin-films are done with the help of FEI Quanta 200, equipped with an Oxford Inca Energy Dispersive X-ray (EDX). Chemical analysis.
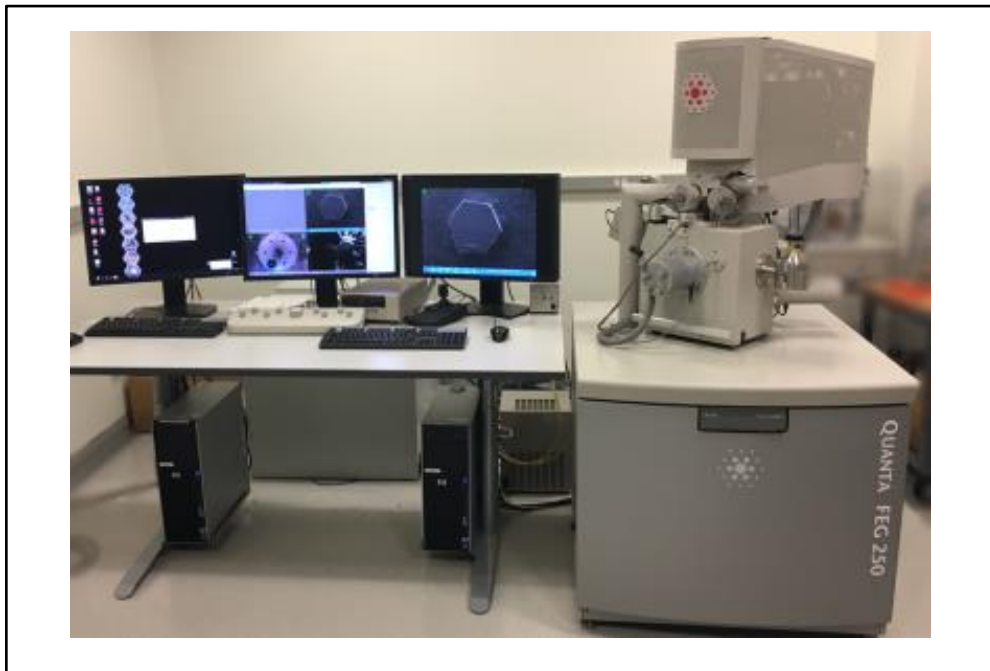
Fig(2.3.5)

Chapter 3: Litlle Iodine is a boon.

In this chapter, I will discuss the hypothesis we formulated in the earlier Chapters of this thesis, the stepwise progress of the work, Result obtained from different characterization techniques used. I have divided this chapter into two parts as I have worked on two different perovskite materials. In first half I will discuss results obtained for $MAPbI_3$ which is most studied Hybrid perovskite solar cell material and build a foundation of the work, in the next half I will discuss most stable and efficient $(FA_{0.83}MA_{0.17})_{0.95}Cs_{0.05}(PbI0_{.83}Br_{0.17})_3$ hybrid perovskite material which is most promising material used in hybrid perovskite solar cells.

3.1 Methylammonium lead iodide (MAPbI₃)

3.1.1 X-RAY Diffraction

X-ray diffraction is one of the fundamental characterization techniques to study the thin-films of perovskites. The study reveals the structure of the material coated on the substrate. Well, crystalline material has more crystals aligned in the same direction resulting in sharp diffraction peaks. In the first set of experiments, I wanted to know-how annealing in the oven, or hot plate affects the crystal formation. $MAPbI_3$ Thin-films the perovskite solution was spin-coated and quenched on the FTO substrate. Then this film is transferred into airtight glass Jar with iodine crystal inside it. The control sample is annealed on hotplate inside the glovebox, whereas the other samples are transferred into the oven with Jar.
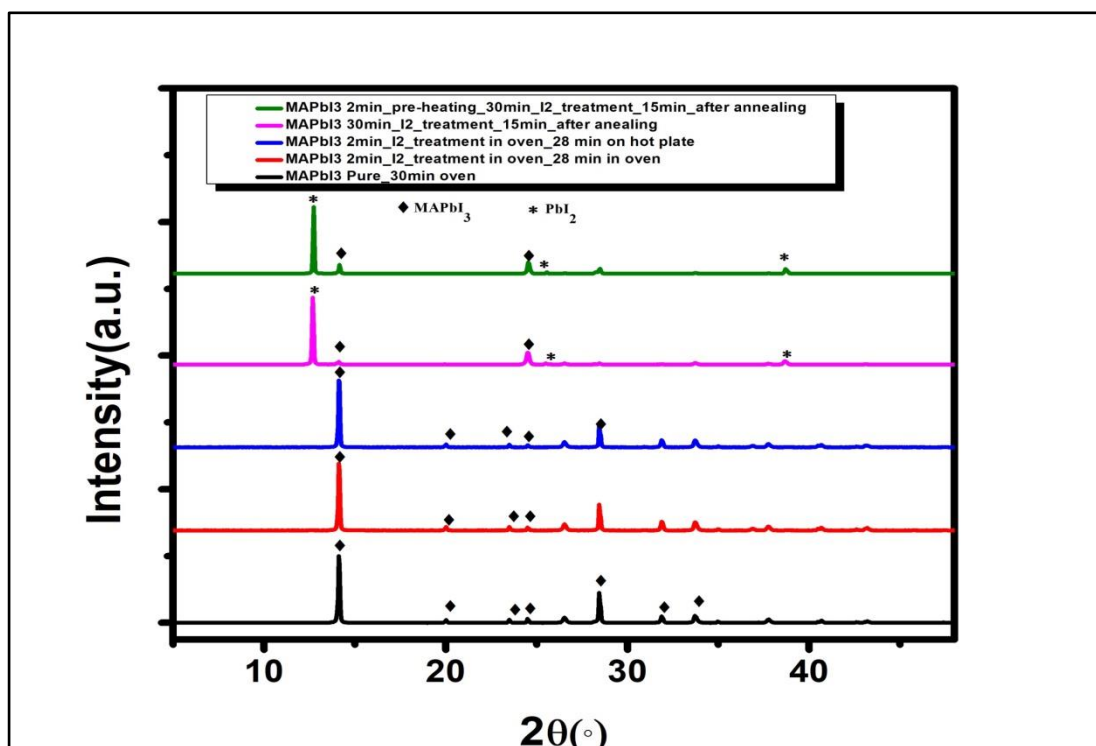
Fig(3.1.1)

The diffraction pattern observed from Fig. (3.1.1) Shows that the longer duration of molecular Iodine treatment results in the formation of PbI_2, which is a non-perovskite phase that can lead to a loss in V_{oc}, J_{sc}, and PCE of the solar cell devices. From this experiment, we also come to know that there is no evident difference between two different annealing methods. So I decided to continue the post-treatment annealing in the glovebox. The table below shows the 2θ ° peak values and hkl plane corresponding to it.

2θ°	hkl
14.01, 14.07	002, 110
19.90	020
23.42	121
24.45	022
28.23, 28.35	004, 220
31.75	222
34.88	024

Table (3.1)

The peaks in the table (3.1) shows peaks corresponding to the formation of the tetragonal phase of $MAPbI_3$. The thin-films of Iodine treated samples looked transparent but dark as well. The findings from the X-ray diffraction pattern prove the presence of the tetragonal perovskite. The thin-film with 2 minutes of iodine treatment was less transparent than the film, which was treated for 30 minutes. As transparency increased, the PbI_2 formation increased; hence, we have to find out optimum treatment time from which we can have a well transparent and complete perovskite film. To optimize it, in the next part of the experiment, I made different samples with different duration of Iodine treatment ranging from 3 minutes to 30 minutes exposure. The x-ray diffraction pattern obtained from the set of the samples is compiled in fig(3.1.2)
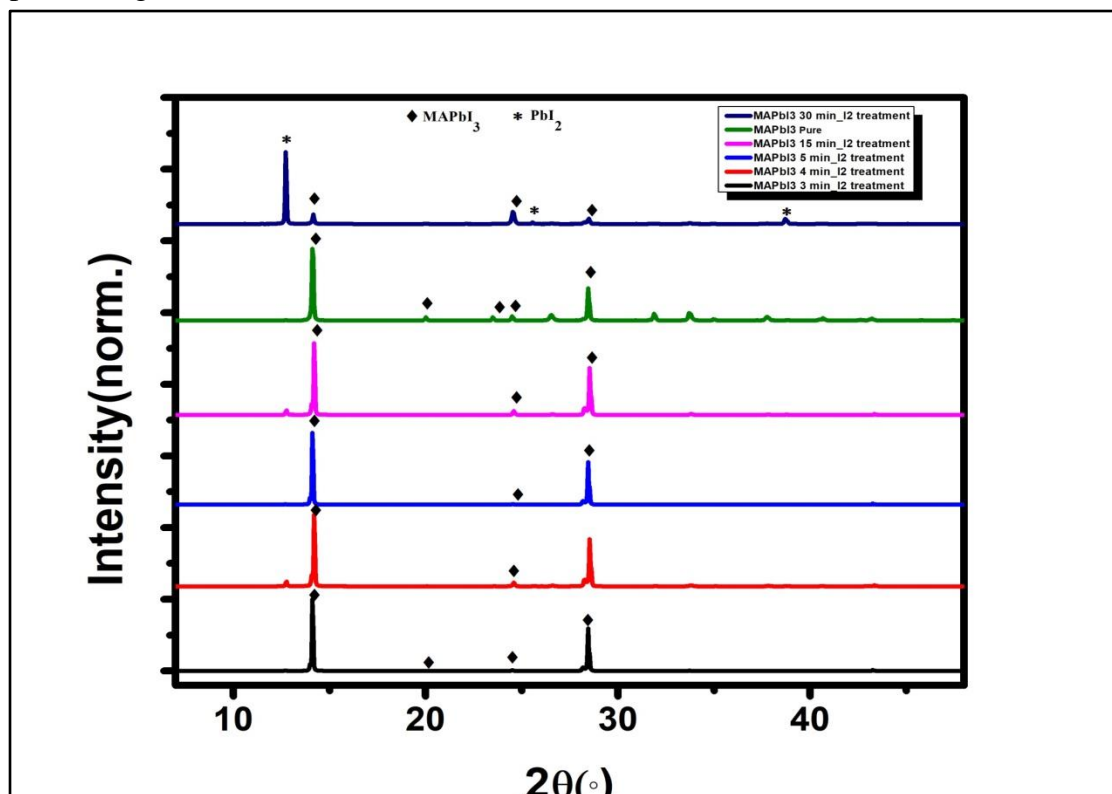
Fig(3.1.2)

Now since I have confirmed the formation Perovskite phase using diffraction pattern, I have t quantified the transmittance by UV-Vis spectroscopy in the next section of this chapter.

3.1.2 UV-Vis spectroscopy

In the first chapter, we have discussed that Hybrid perovskites are materials with a very high absorption coefficient, which makes them one of the best contenders in solar cell applications. The transmittance of the samples is measured in the integrating sphere since, without sphere, the output has a lot of noise, which overshadows the signal from the material. The transmittance without the integrating sphere is shown in fig. (3.1.3a)
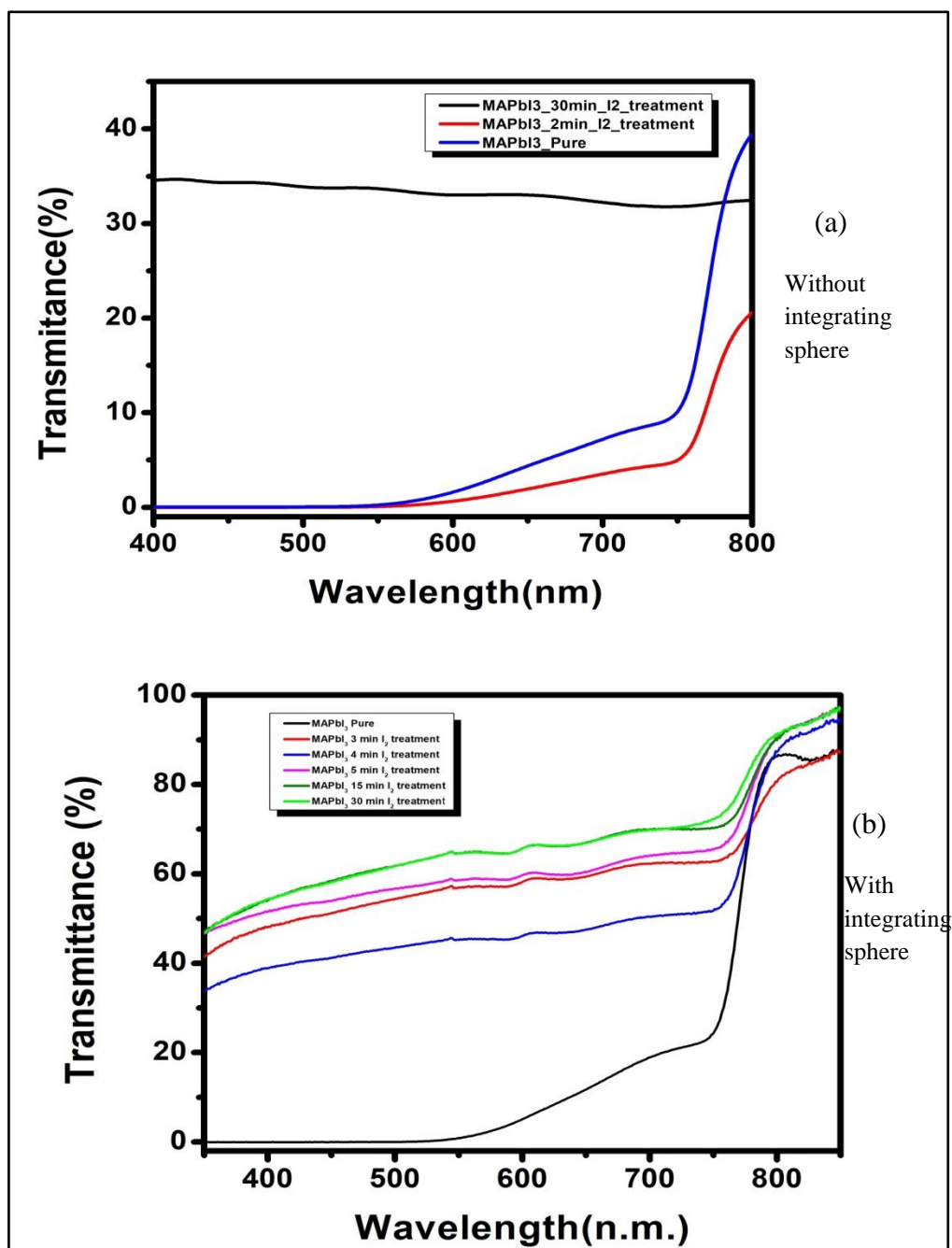
Fig(3.1.3)

The straight line in the transmittance scan shows overshadowing by noise.Fig.(3.1.3b) Shows the exact transmittance that follows a trend of increasing transmittance with increasing time of treatment. The absorption tail of these samples appears around 470 n.m. to 480n.m. hence, the excitation wavelength used for steady-state photoluminescence is 475n.m. we excite with higher energy than bandgap to obtain weak traceable signals as well.

3.1.3 Steady-state Photoluminescence spectroscopy

Photoluminescence is measured on FLS-980, with Xenon lamp as a source. Fig. (3.1.4a) Consist of the normalized photoluminescence of the thin-films. The emission peak varies from the standard perovskite, which is around 774n.m.

(a)   (b)
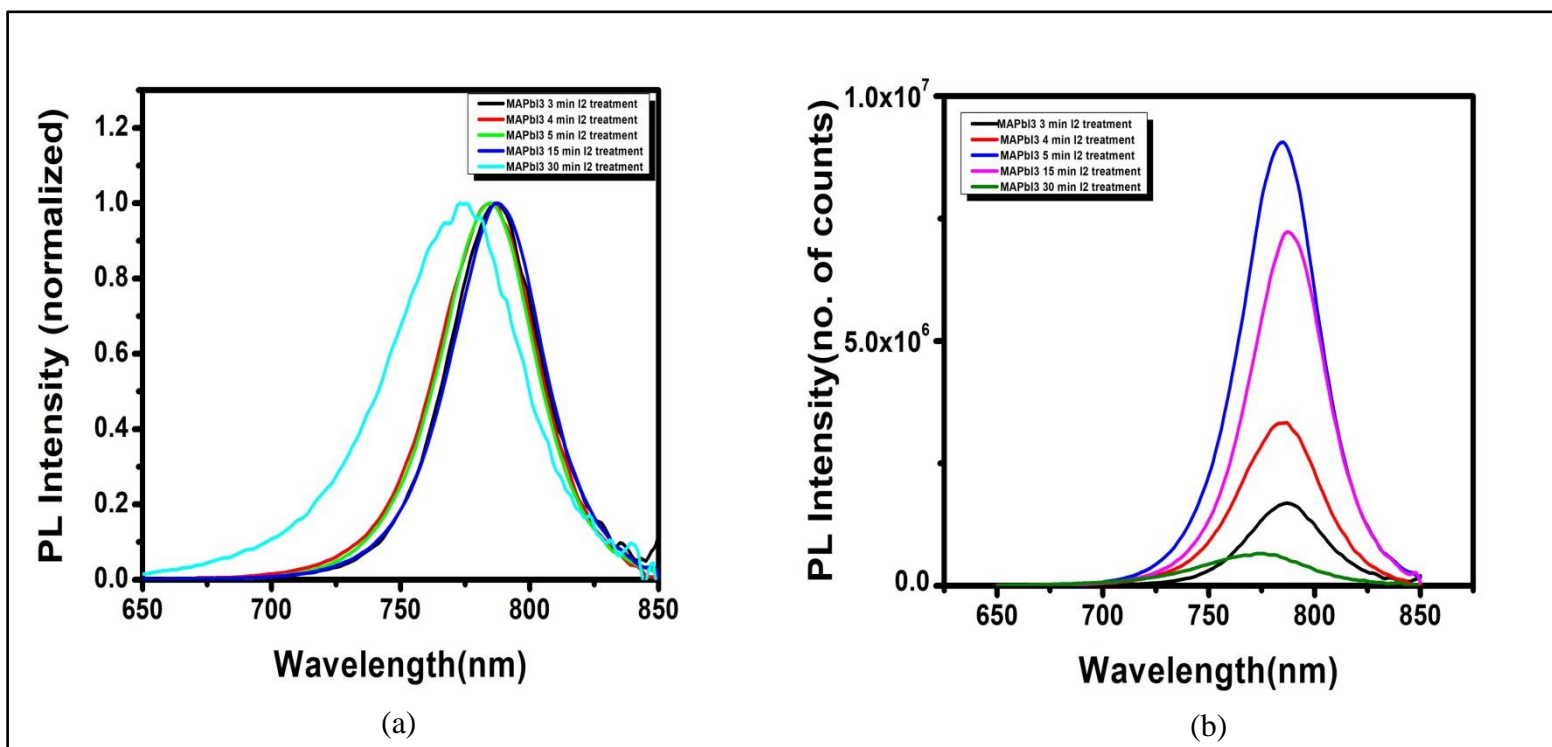
Fig(3.1.4)

Increasing the iodide treatment duration shifts emission peak towards higher photoluminescence energies. Fig. (3.1.4b) Has nonnormalized PL intensities. The highest PL counts in 5 minutes Iodine treatment sample supports the absorbance analyzed from transmittance spectra in the previous section of this chapter. Exposure to the iodine vapors for a longer duration is not good since the photoluminescence is seen to be quenching, with the broadening of the emission peak is also observed. One of the main reasons behind very high PL count could be because of photon recycling and could be confirmed by PLQY of the thin films for further clarification on the nature of the emission.

3.1.4 Photoluminescence lifetime measurement

The photoluminescence lifetime is measured on Time correlated single photon counting setup of FLS980 with 775nm excitation wavelength.
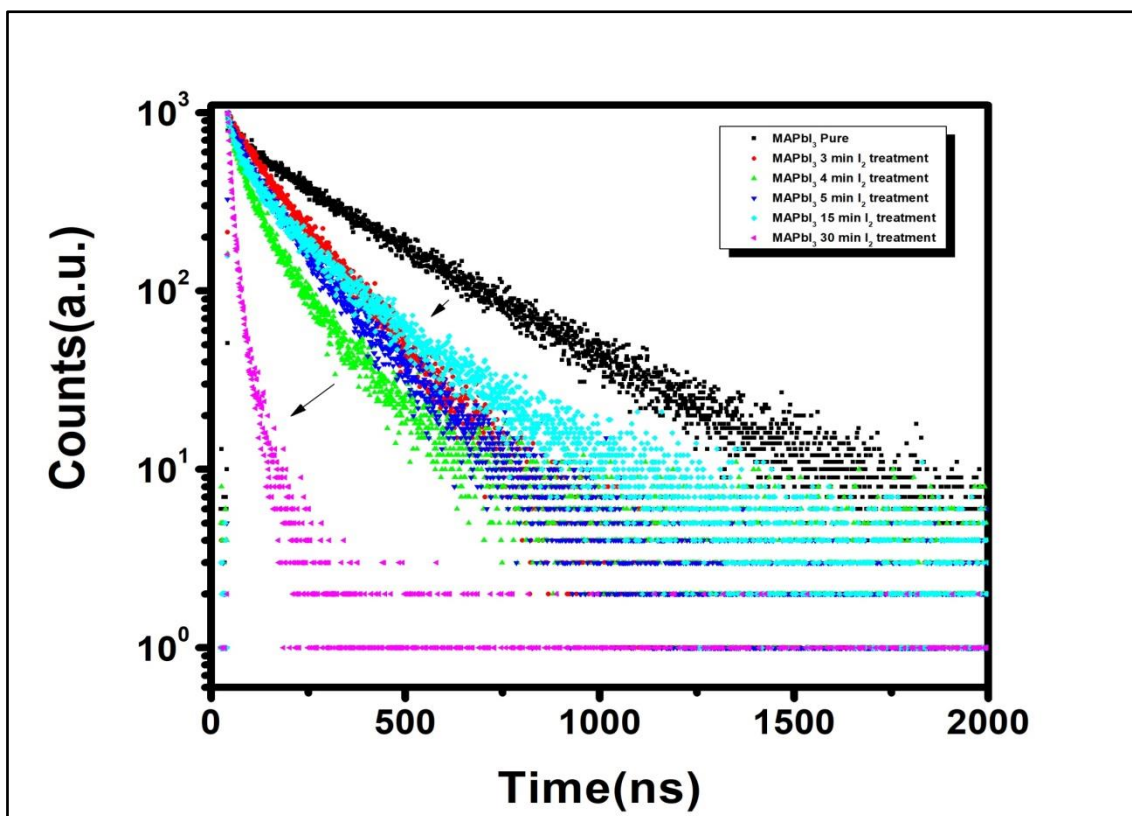
Fig(3.1.5)

One of the exciting things I have observed in Lifetime decay is a sample with 15 min I_2 thin-film has longer decay time than 3 min and 4 min samples if we compare the results with non-normalized Photoluminescence spectra, we see higher PL counts in 15 min sample than 3 and 4 minutes samples. Another exciting trend is as treatment time increased, the decay time started decreasing but suddenly increased in between and again reduced. The reason behind the trend could be found out by more fundamental studies of the above samples.

3.1.5 SEM and Elemental mapping

Scanning electron microscopy is performed to identify the reason behind Transparent perovskite Thin-films. The thin films are mounted on the stub and put under a high vacuum. The images are taken in two different magnification so that we can compare grain size and shapes. Image 1 in fig. (3.1.6) Shows uniform sized grains with around 300n.m. size. The morphology in image 1 is compact and smooth. Image 2 is of 3-minute iodine treatment sample, the sharper and bugger grains with needle shapes are found on the surface. Earlier it was thought that the space between two needles is empty and covered by FTO glass substrate, but the EDX mapping shows a thin layer of Perovskite as well. Image 3 shows similar

features like Image 2 but sharper. The grains in Image 4 are bigger than grains in earlier samples with almost entirely formed needle shapes.
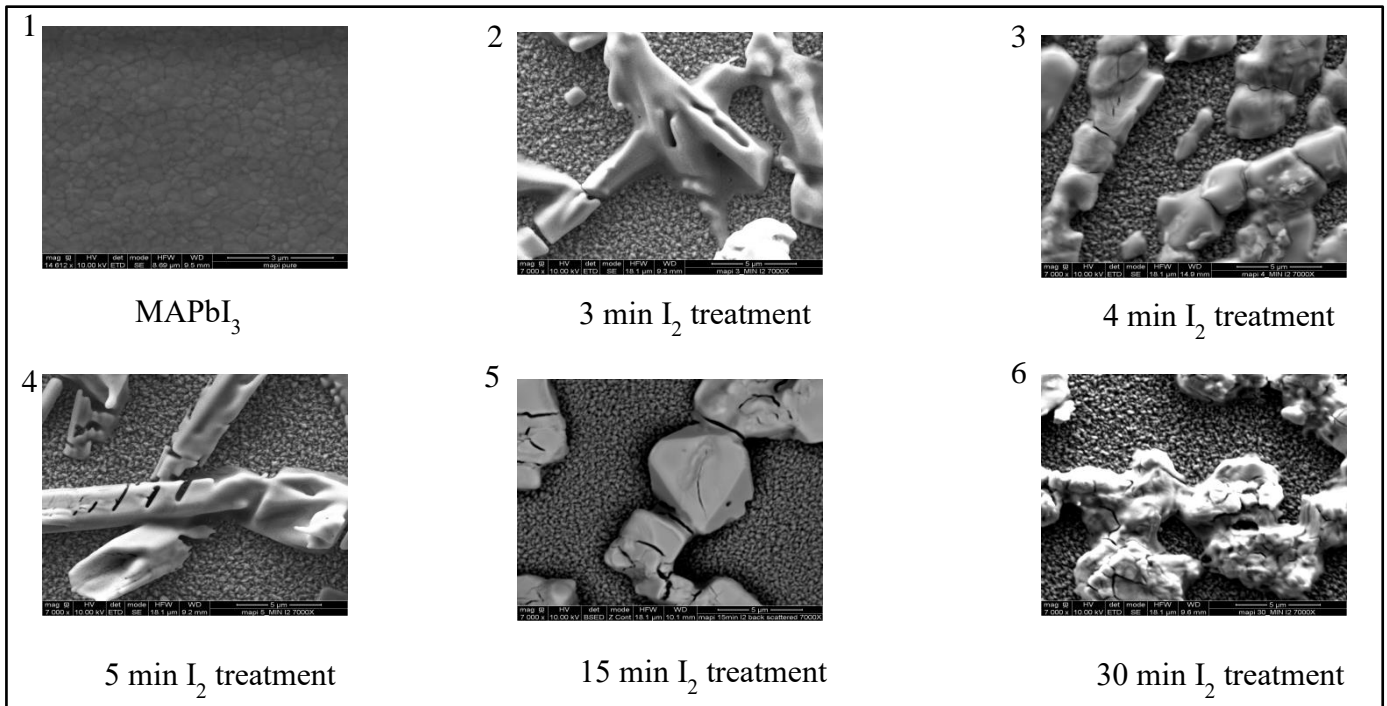
Fig(3.1.6)

Grains in Image 5 have an entirely different shape than Image 4 and look like well-formed grains with a smooth surface. Image 6 shows non-uniform grain shape and rough grain surface, indicating degradation. We will discuss EDX mapping below
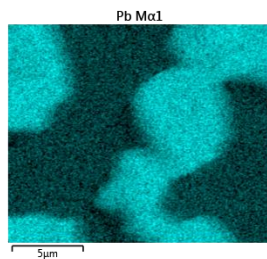

MAP-1

4 minutes Treatment

5μm

C Kα1_2   Pb Mα1   I Lα1   Sn Lα1   O Kα1

5μm   5μm   5μm   5μm   5μm

MAP-2

5 minutes Treatment

25μm

C Kα1_2   Pb Mα1   I Lα1   Sn Lα1   O Kα1

25μm   25μm   25μm   25μm   25μm

MAP-3

15 minutes Treatment

5μm

C Kα1_2   Pb Mα1   I Lα1   Sn Lα1   O Kα1

5μm   5μm   5μm   5μm   5μm

MAP-4

35
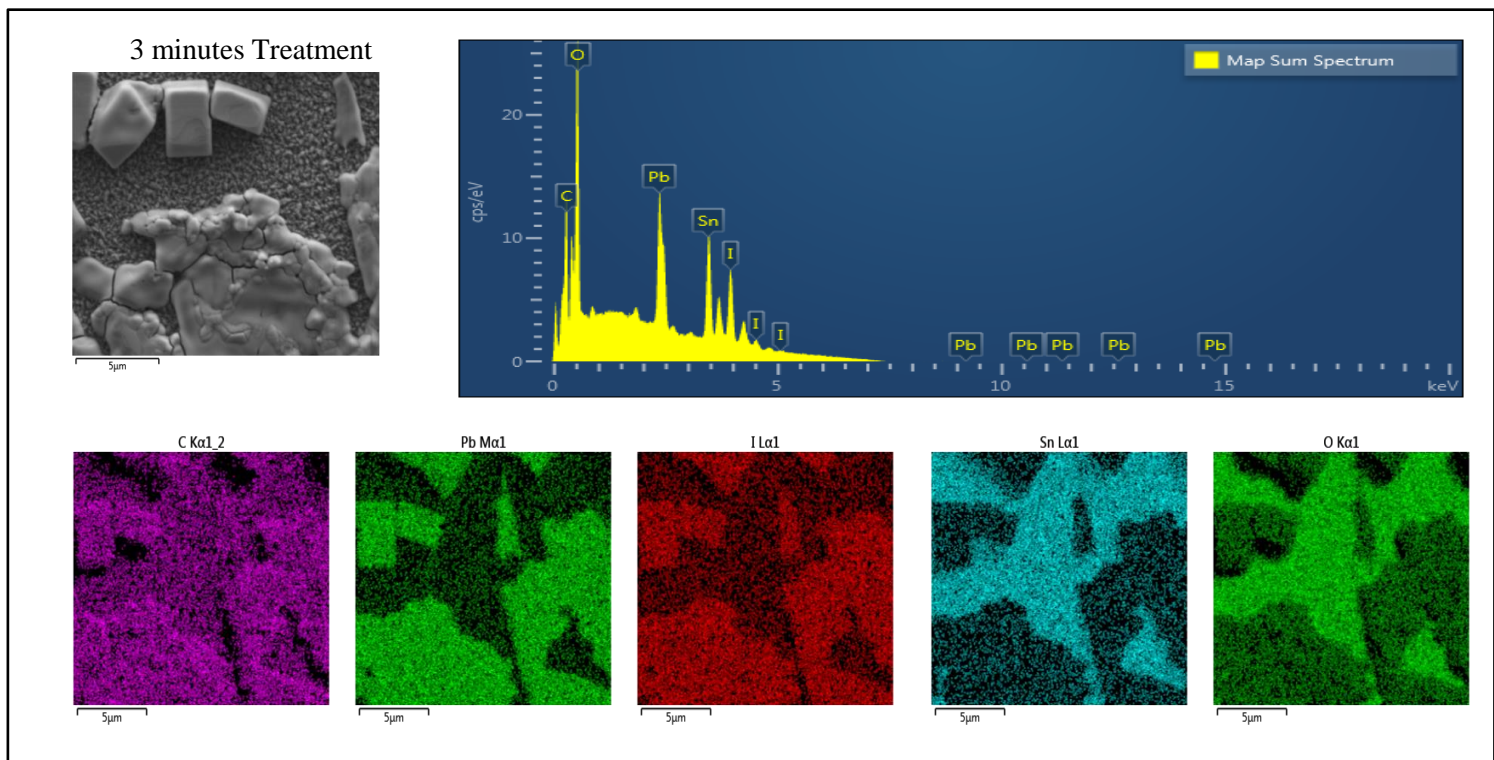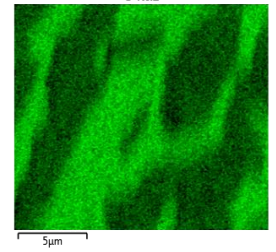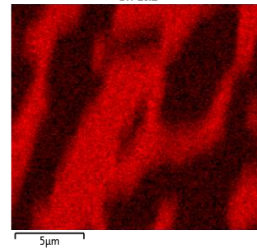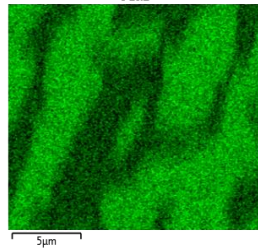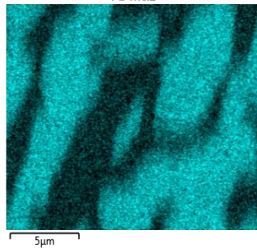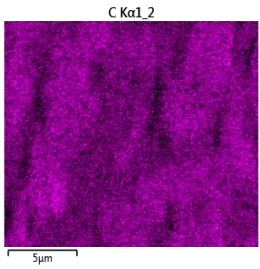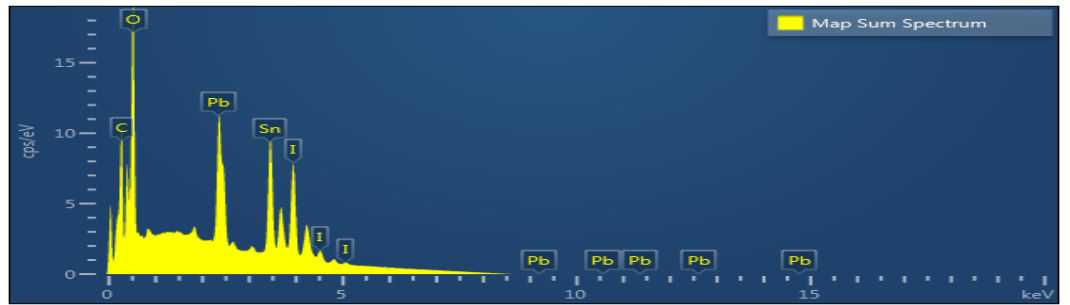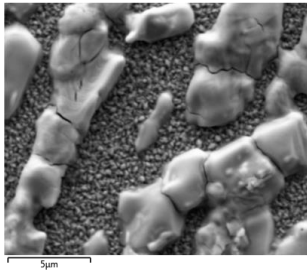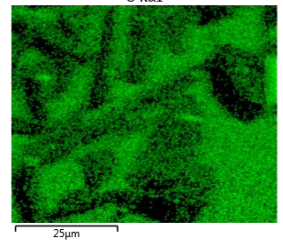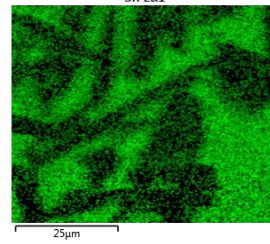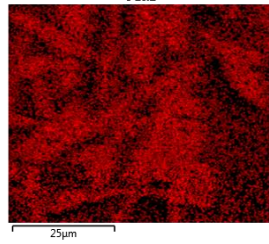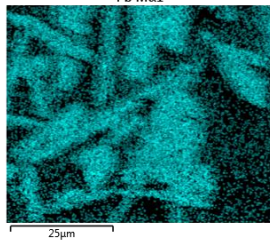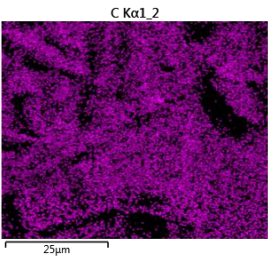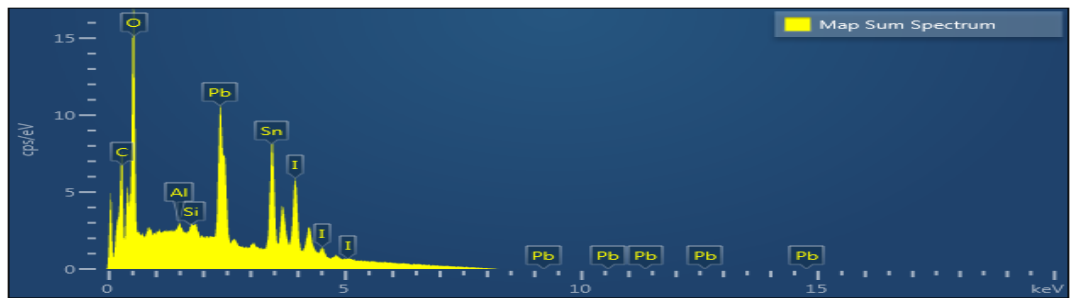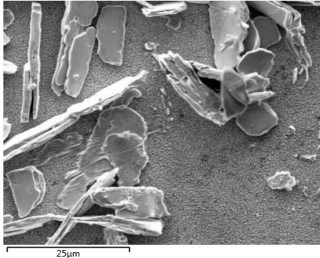
30 minutes Treatment
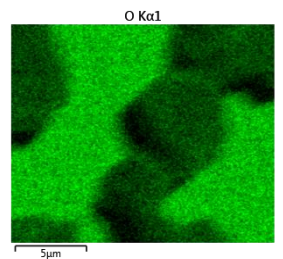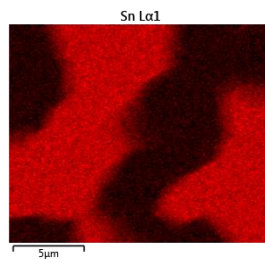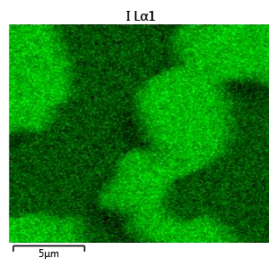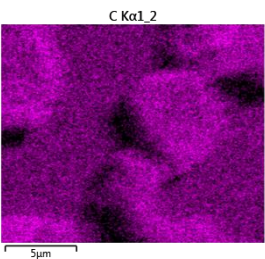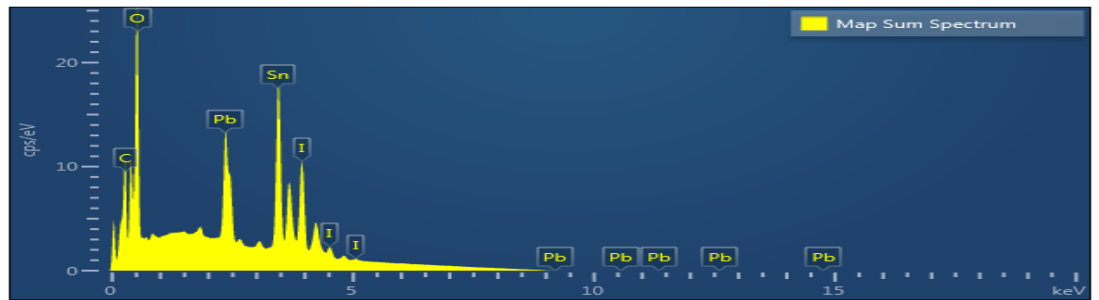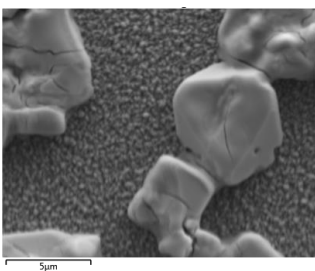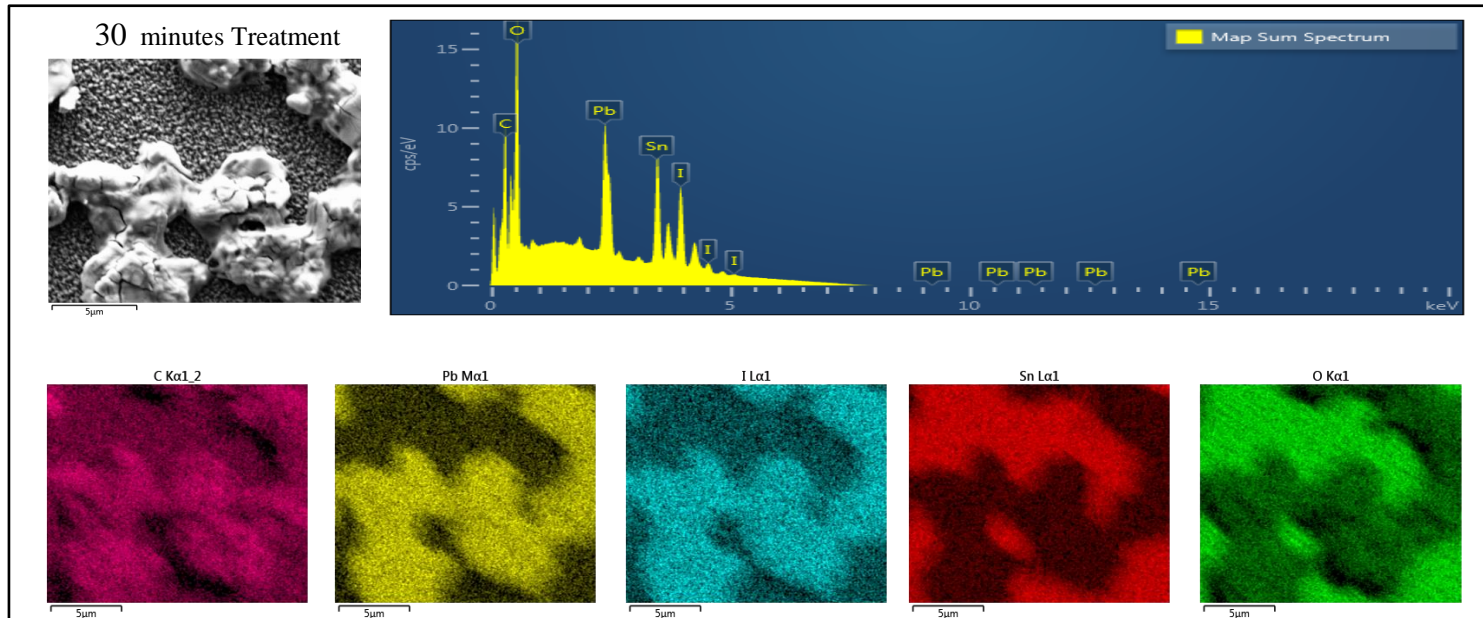
MAP-5

We confirm the different grain shape, size, and the presence of a thin layer of perovskite material between two big grains.

The obtained results from the above characterizations are new findings and could be useful in Economic, transparent, and stable perovskite solar cells. In the next section of this chapter, I have tried the same experimental characterization to see if we can make a Highly efficient transparent perovskite solar cell, Using material with Highest reported PCE and stability in perovskites.

3.2 Mixed cation-halide Perovskite $((FA_{0.83}MA_{0.17})_{0.95}Cs_{0.05}(PbI_{0.83}Br_{0.17})_3)$

3.2.1 X-RAY Diffraction

The first trial of the work was to test if it is possible to get transparent thin-films with triple cation perovskite. In this experiment, I have studied the diffraction patterns obtained from different samples that have different duration of treatment. Fig. (3.2.1) shows diffraction patterns and peaks corresponding to different phases of the material.

$2\theta°$	Phase of material
11.4	δ -FAPbI$_3$
12.6	PbI$_2$
14.1	α -Perovskite
19.88	α -Perovskite
24.5	α -Perovskite
25.6	PbI$_2$
26.46	δ-FAPbI$_3$
28.41	α -Perovskite
40.05	PbI$_2$

Table (3.2)
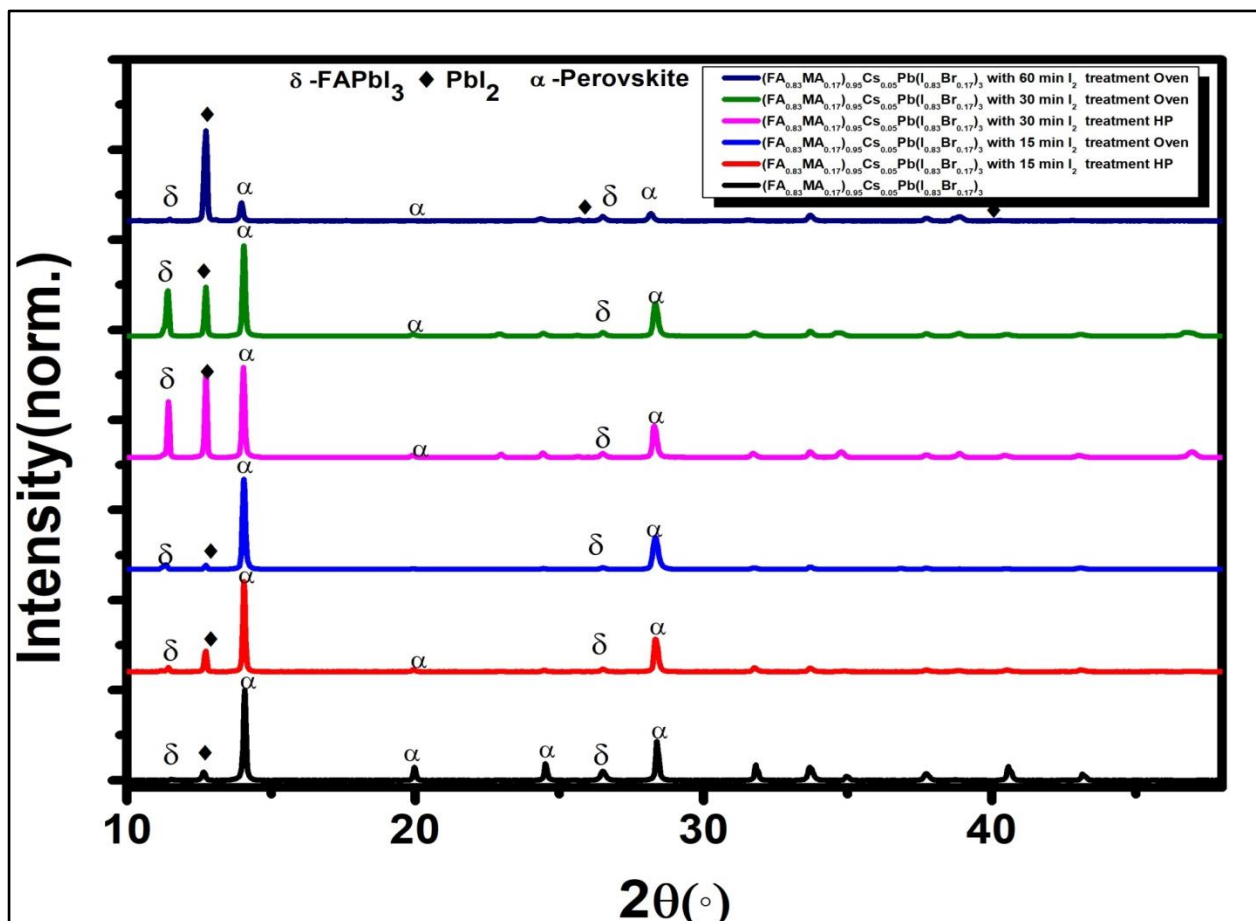
Fig (3.2.1)

From the diffraction pattern, I have obtained from the new material shows that PbI_2 formed during the treatment in the oven is less than treatment in samples treated on Hotplate. I have also observed the formation of the non-perovskite δ- phase of $FAPbI_3$.It is evident from the diffraction pattern that a longer duration of exposure leads to non-perovskite pashes. The Interesting point is the thin-films in this experiment are transparent as well. I have to confirm a similar trend observed in $MAPbI_3$. The transmittance is measured by UV-Vis spectroscopy and is discussed in the next section.

3.2.2 UV-Vis spectroscopy

In an experiment performed in (section 3.1.2), I have already come to know that the thicker film scatters more light; because of that, I reduced the thickness of the perovskite material by increasing the rpm of spin-coating and diluting the precursor solution. Since I have performed an earlier experiment with the integrating sphere, I have to perform this part with the integrating sphere as well. In fig. (3.2.2) The transmittance of the perovskite thin-films on the FTO/Glass substrate is plotted. The transmittance follows a similar trend like $MAPbI_3$, and after a few more characterizations, It will be clear where this work will proceed. The fi. (3.2.3) shows the transmittance of Thin-film with a blocking layer, Mesoporous TiO_2, and Perovskite layer on top of all.

37
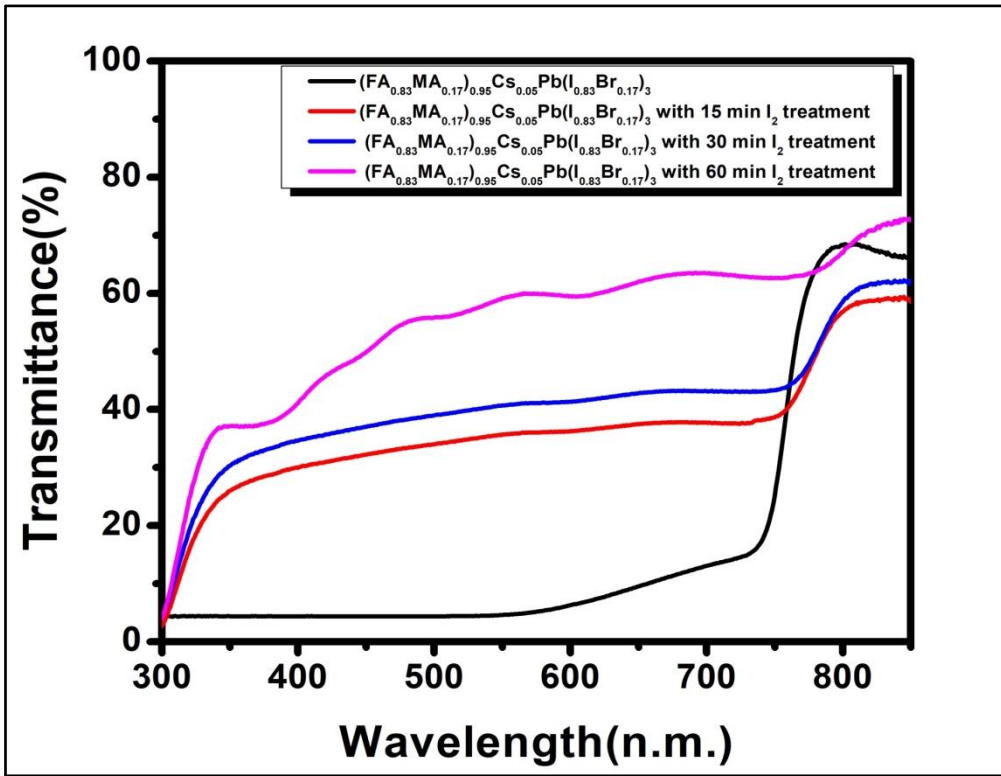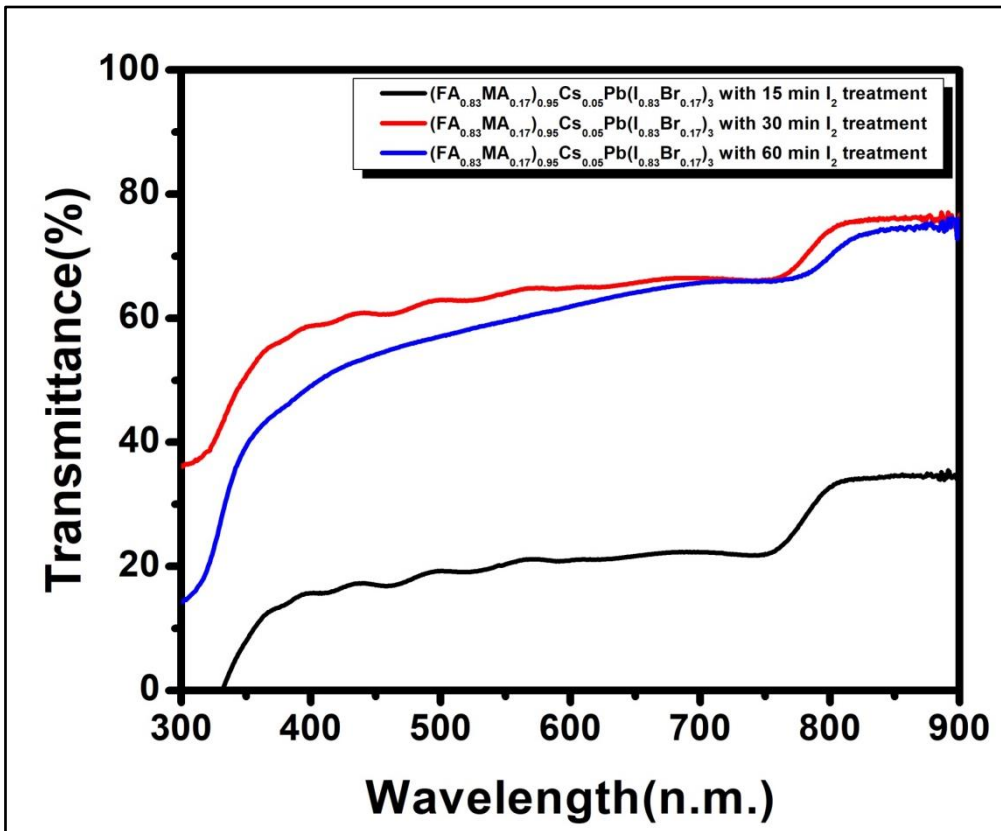
Fig (3.2.2)

Fig (3.2.3)

It is interesting to see the transmittance of the thin-films is still maintained with the ETL and blocking layer.

3.2.3 Steady-state Photoluminescence spectroscopy

Samples with different duration and methods of treatment used to measure Photoluminescence. It was surprising to see the huge difference between samples prepared using the Oven and Hot plate method. Thin-film annealed in an oven has broader emission at a higher wavelength.
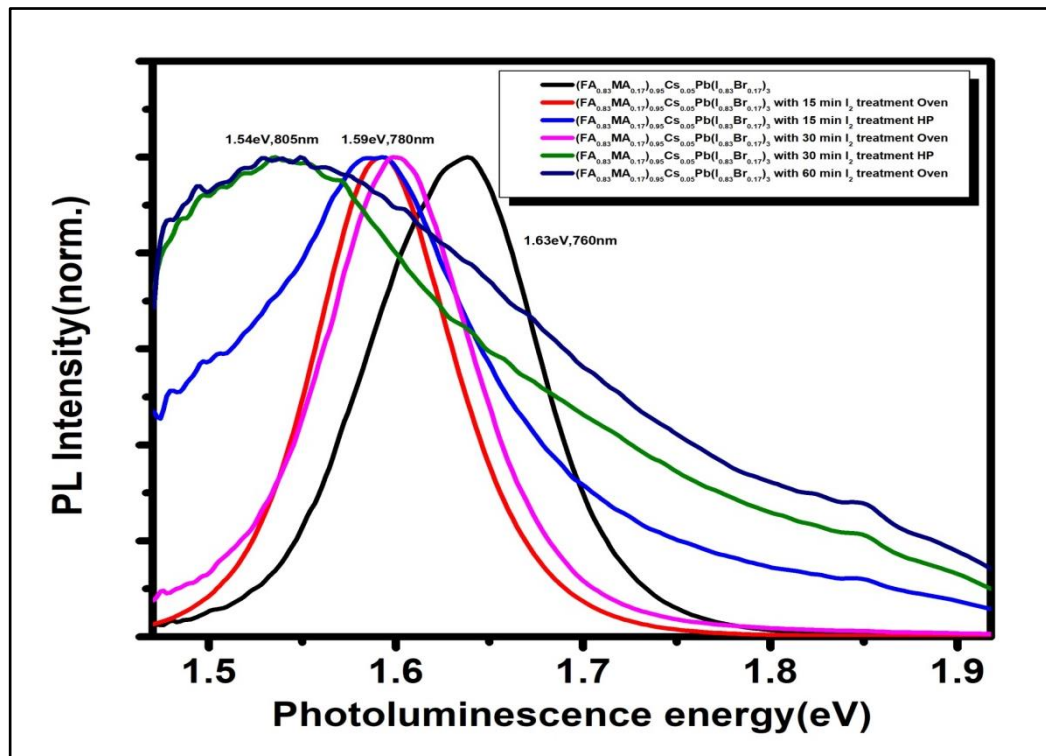

Fig (3.2.4)

3.2.4 Photoluminescence lifetime measurement

The same setup, which was used in section (3.1.4), is used here.

Fig (3.2.5)

39
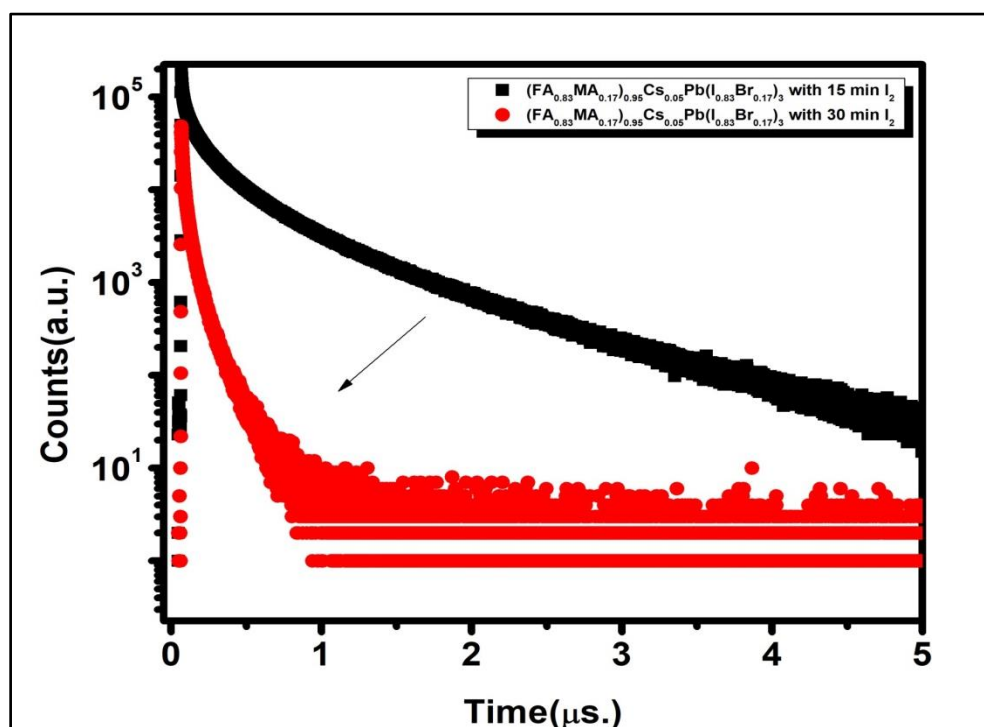
A similar trend is observed in this characterization as well, increasing the Iodine exposure decreases the Photoluminescence lifetime, creating more defects. These defects contribute towards the non-radiative losses.

3.2.5 SEM and Elemental mapping

The samples with two different sets are characterized using scanning electron microscopy. In the first part, I have characterized Triple cation perovskite thin-films spin-coated on FTO/glass substrate. In the next part of the experiment, the half device cell is characterized to observe the morphological evolution of the thin-film.
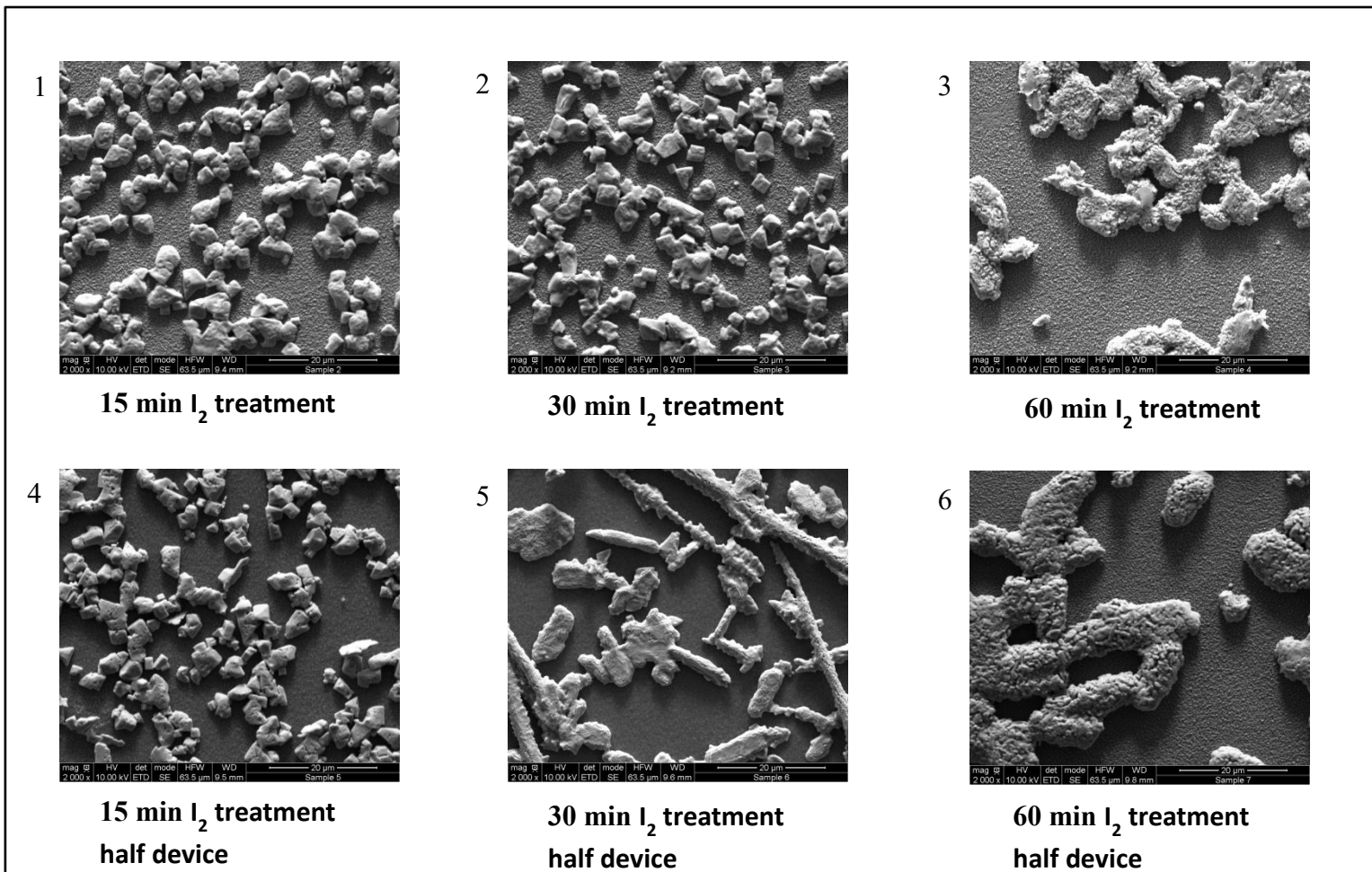
Fig (3.2.6)

While comparing image 1 and image 2, it is challenging to differentiate between them, but since the morphology is almost similar, but image 3 shows severe degradation with rough grains. All these are spin-coated on the FTO substrate. On the other hand, the image 4, and image 5 has utterly different morphology, the grains in image 4 are well-formed with a smooth surface, whereas the grains in image 5, are large rod-like structures. From these

specific shaped structures we can conclude that there is some driving force working in the presence of Iodine that leads to the formation of rod-like structures.

Elemental mapping using EDX

Elemental analysis is necessary to quantify, the uniform morphology of the perovskite absorber layer on the substrate, we can also know if there are contours if the material is degraded.
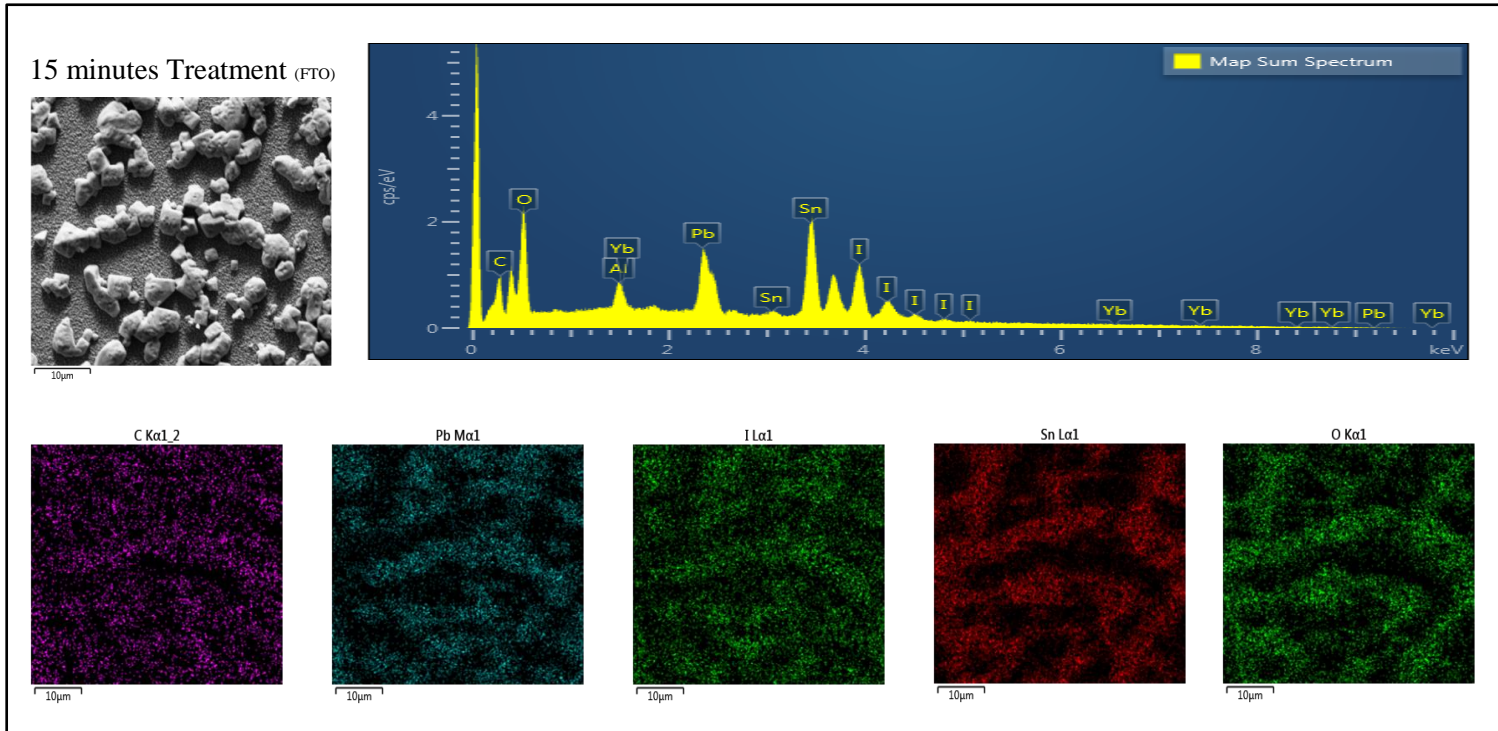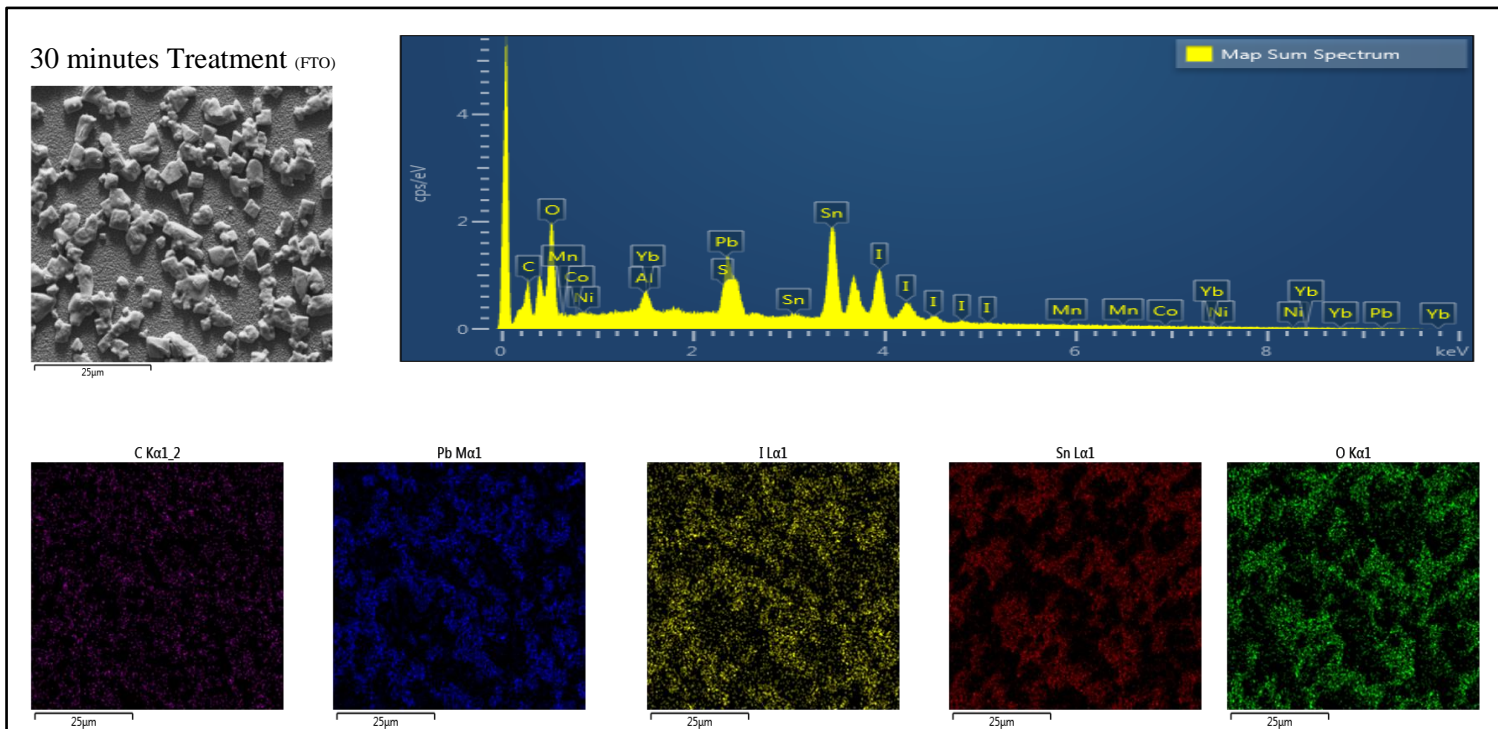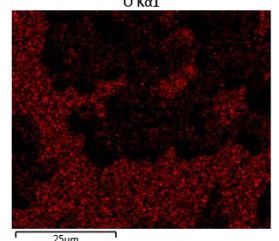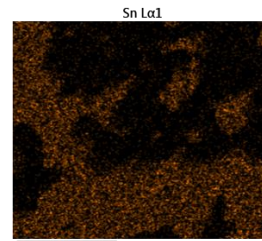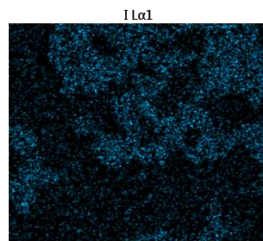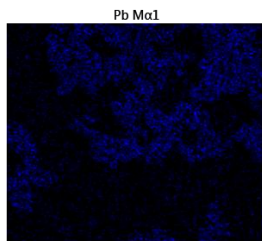
15 minutes Treatment (FTO)

MAP-6

30 minutes Treatment (FTO)

MAP-7

60 minutes Treatment (FTO)

C Kα1_2   Pb Mα1   I Lα1   Sn Lα1   O Kα1

MAP-8

15 minutes Treatment (Device)

C Kα1_2   Pb Mα1   I Lα1   Br Lα1,2   Sn Lα1   O Kα1

MAP-9

30 minutes Treatment (Device)

C Kα1_2   Pb Mα1   I Lα1   Sn Lα1   O Kα1

42   MAP-10
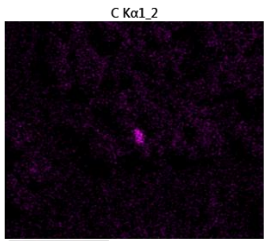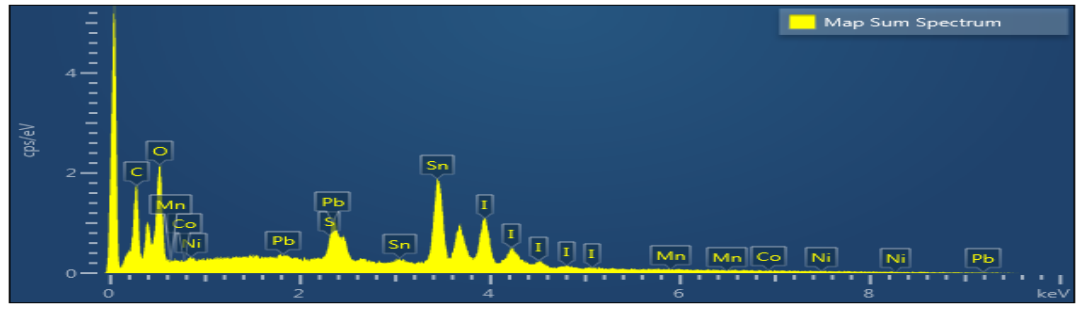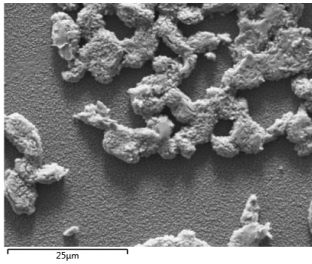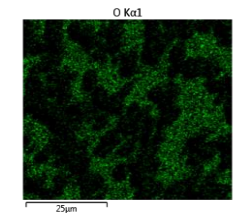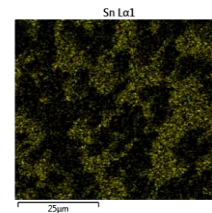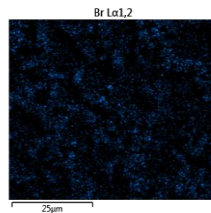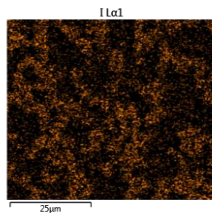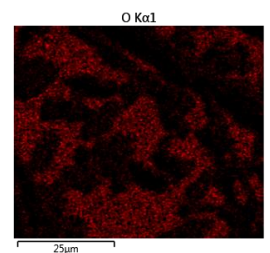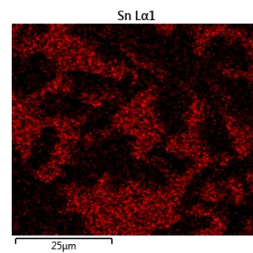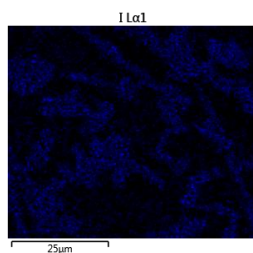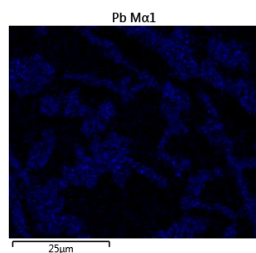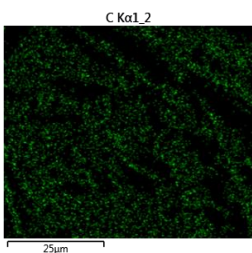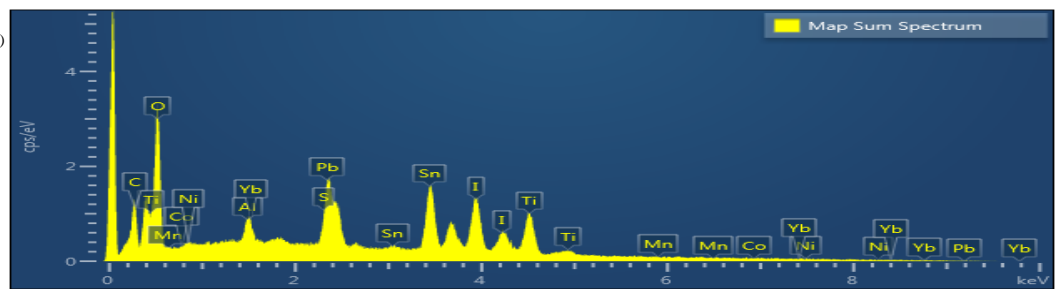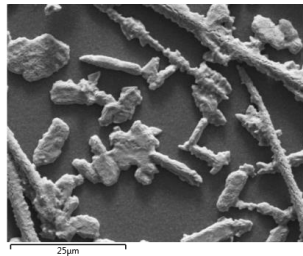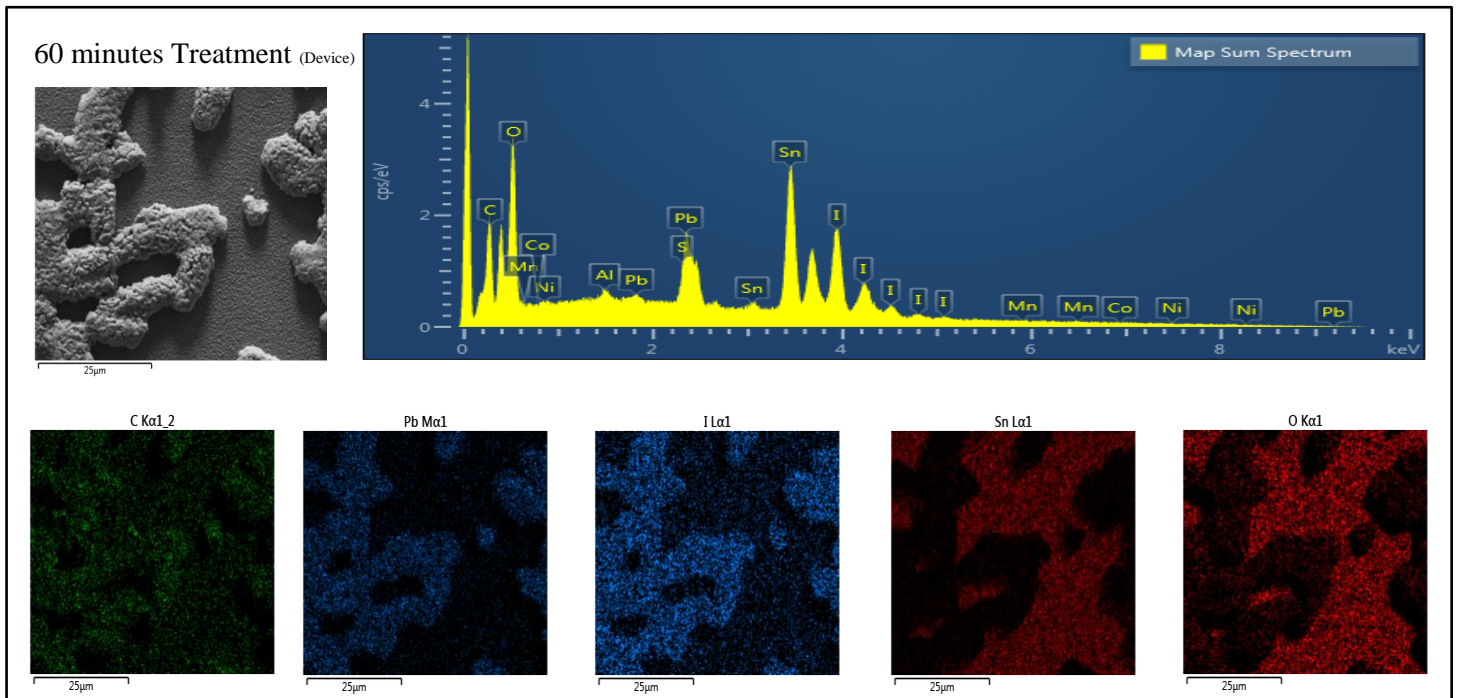
MAP-11

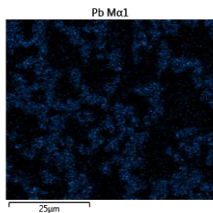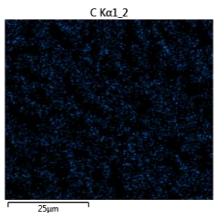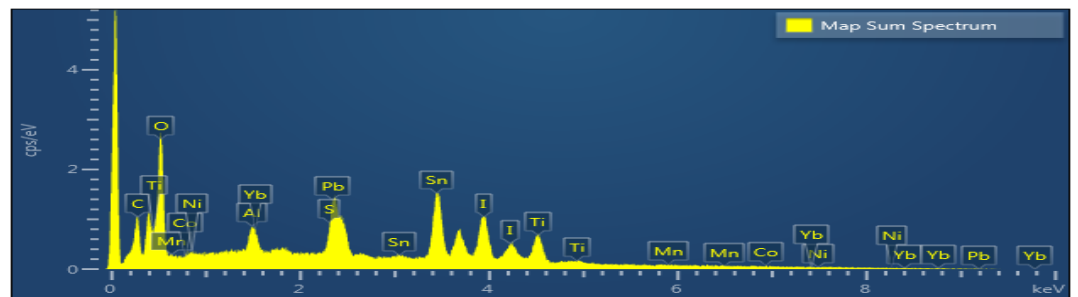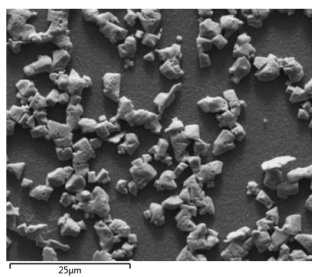It is evident from EDX mapping that the transmittance of the thin-film is because of the morphology of the Thin-films. As the treatment time increases, the void size increases, also after some threshold time, the Iodine starts to form PbI_2. The voids can be eliminated by further optimization of the thickness of the perovskite and duration of the Iodine treatment. The results are discussed in the next chapter of the thesis, where I will be comparing my results with earlier reports and how the different characterization techniques support my Hypothesis.

3.2.6 Device for dark current measurement

We all know from previous reports that the presence of the voids in thin-films can reduce the fill factor drastically which can hamper the Final PCE of the solar cell device since we confirmed large grain size from SEM imaging, we wanted to try some solar cell devices, the device was fabricated following the well-studied protocol. [21]

In the presence of voids, the HTM leaks through the Perovskite layer, due to contact between HTM and mesoscopic TiO_2 the recombination occurs at interface and device is short-circuited.
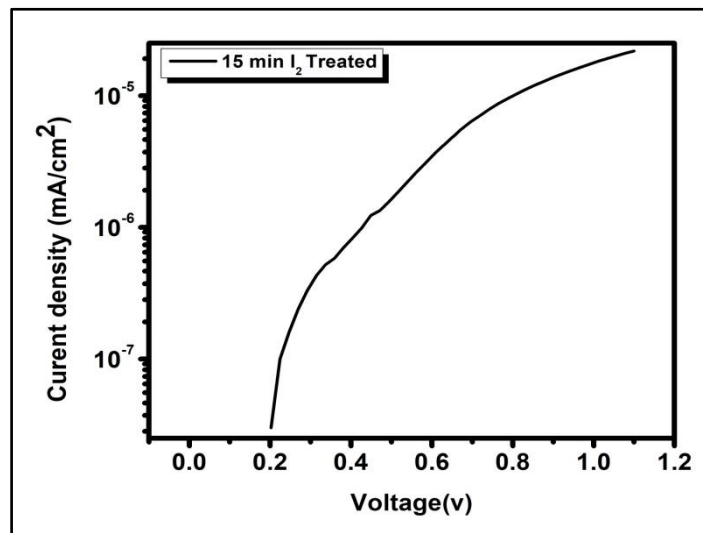
Fig. (3.2.7)

Chapter 4: Discussion,Conclusion & Future perspective of the work

4.1 Discussion

The initial motivation for this work was to make a highly stable and efficient perovskite solar cell. I planned to achieve the same by passivating Iodine defects, which are still one of the most critical defects due to its self destructing nature. In the previous reports, Yabing Qi *et al.* have studied the degradation by iodine and concluded that the Iodine triggers the degradation mechanism in perovskites when already formed perovskites are treated with iodine vapor. Fan Fu *et al.* have proposed a pathway of self-degradation mechanism in their recent work. They claim this degradation occurs independently of the sample preparation method. [22] There also have been reports of the use of Iodine as a passivating agent in precursor solution[20] from Yang *et al.* The recent work by Tarasov *et al.* also shows Iodide assisted the formation of perovskite by treating Perovskite precursor deposited thin-film with iodine vapor at ambient temperatures. [23]

If we compare the results of my experiment above experiments, there are some results that I have seen in my experiment, as well. Like the longer duration of iodine treatment degrades perovskite, which is similar to Yabing Qi results, But formation larger grains under iodine vapor matches with Tarasov's results. Fan Fu's work claimed that independent sample preparation method Iodine driven degradation is observed in their experiment at 80°C, but In my results, the lead iodide formation negligible in case of shorter duration of exposure with transparent thin-films. And highly oriented crystals.

I want to discuss the mechanism because it can widen our understanding of these materials. The transparent films which I observed in this experiment are becoming transparent because iodine is playing as a driving force for the formation of a highly crystalline film with well-oriented crystals. When thin-films are getting spin-coated, during the quenching by antisolvent, half of the perovskite is already formed as we instantly see a color change. When this film is transferred in Glass jar with iodine, the film becomes dark, and after few minutes of annealing in the iodine atmosphere, it becomes yellowish dark during the post-annealing process at110°C the excess of iodine which has occupied some space in bulk perovskite, leaves the structure. The removal of excess iodine from perovskite, the voids are left behind, which brings the transparent nature to the thin-film. It is also observed that the thin-films are still stable after 1968 hours.

4.2 Conclusion

In this thesis, I tried to compile all aspects of the solar cells from history, working principles, challenges, new strategies, and new conflicts. From all the results obtained from characterizations and other work reports, I conclude that if the perovskite is treated with iodine vapor when all the precursors are in their initial stage of forming perovskites then Iodine can help to passivate the iodide defects a well as MA defects due to mismatch mechanism, since their ionic radii are relatively similar. It is also necessary to treat these thin-films with passivating molecules like iodopentaflurobenzene to stop the migration of iodine under an electric field. I wish to probe into the dynamics of this process. It is found that iodide defects occur at the grain-boundaries, from SEM images I have observed merging of the grains to form larger and well-ordered grains, it is possible that Iodine playing a crucial role in binding these grains in a particular manner. To prove this, I have to perform HRXPS, RAMAN, and more characterization, which can give more insights into the material.

4.2 Future perspectives

The transparent thin-films of the perovskites interests many as it has a wide variety of applications ranging from smart windows to Tandem solar cells. The primary purpose of this work is to improve the longterm stability and understand the degradation mechanism properly; the more insights into the degradation mechanism will help us to come up with new and more efficient strategies. The optimization of solar cell devices will be done in the next part. To deal with the sort circuiting because of voids, I have come up with an idea of using non conducting Al_2O_3 as a mesoscopic layer, so even if the HTL leaks into perovskite layer and mesoporous layer, there won't be any recombinations. We are going to use polymer-based HTM to overcome the conductivity lost during the formation of the voids.

It will be tough to conclude everything about this process with whatever characterizations I have.

'Science doesn't just run according to a hypothesis; the journey of understanding it drives it further.'

References

1) R. F. Pierret, Advanced semiconductor fundamentals. (Addison-Wesley Publishing Company, Reading, 1987)

2) B. G. Streetman and S. K. Banerjee, Solid-state electronic devices. (Pearson Education, New Jersey, 2006), 6th edition

3) Polman, A., Knight, M., Garnett, E., Ehrler, B. and Sinke, W. (2016). Photovoltaic materials: Present efficiencies and future challenges. *Science*, 352(6283), pp.aad4424-aad4424.

4) NREL efficiency chart (accessed: 2019-03-08)

5) ROOKSBY, H. (1945). Compounds of the Structural Type of Calcium Titanate. *Nature*, 155(3938), pp.484-484.

6) Yin, W., Shi, T. and Yan, Y. (2014). Unusual defect physics in CH3NH3PbI3 perovskite solar cell absorber. *Applied Physics Letters*, 104(6), p.063903.

7) Dong, Q., Fang, Y., Shao, Y., Mulligan, P., Qiu, J., Cao, L. and Huang, J. (2015). Electron-hole diffusion lengths > 175 μm in solution-grown CH3NH3PbI3single crystals. *Science*, 347(6225), pp.967-970.

8) Kojima, A., Teshima, K., Shirai, Y. and Miyasaka, T. (2009). Organometal Halide Perovskites as Visible-Light Sensitizers for Photovoltaic Cells. *Journal of the American Chemical Society*, 131(17), pp.6050-6051.

9) Yu, D., Hu, Y., Shi, J., Tang, H., Zhang, W., Meng, Q., Han, H., Ning, Z. and Tian, H. (2019). Stability improvement under high efficiency—next stage development of perovskite solar cells. *Science China Chemistry*, 62(6), pp.684-707.

10) Pazos-Outón, L., Xiao, T. and Yablonovitch, E. (2018). Fundamental Efficiency Limit of Lead Iodide Perovskite Solar Cells. *The Journal of Physical Chemistry Letters*, 9(7), pp.1703-1711.

11) Shockley, W. and Read, W. (1952). Statistics of the Recombinations of Holes and Electrons. *Physical Review*, 87(5), pp.835-842.

12) Kato, Y., Ono, L., Lee, M., Wang, S., Raga, S. and Qi, Y. (2015). Silver Iodide Formation in Methyl Ammonium Lead Iodide Perovskite Solar Cells with Silver Top Electrodes. *Advanced Materials Interfaces*, 2(13), p.1500195.

13) Wang, S., Jiang, Y., Juarez-Perez, E., Ono, L. and Qi, Y. (2016). Accelerated degradation of methylammonium lead iodide perovskites induced by exposure to iodine vapour. *Nature Energy*, 2(1).

14) Shao, Y., Xiao, Z., Bi, C., Yuan, Y. and Huang, J. (2014). Origin and elimination of photocurrent hysteresis by fullerene passivation in CH3NH3PbI3 planar heterojunction solar cells. *Nature Communications*, 5(1).

15) Lin, Y., Chen, B., Zhao, F., Zheng, X., Deng, Y., Shao, Y., Fang, Y., Bai, Y., Wang, C. and Huang, J. (2017). Matching Charge Extraction Contact for Wide-Bandgap Perovskite Solar Cells. *Advanced Materials*, 29(26), p.1700607.

16) Wen, T., Yang, S., Liu, P., Tang, L., Qiao, H., Chen, X., Yang, X., Hou, Y. and Yang, H. (2018). Surface Electronic Modification of Perovskite Thin Film with Water-Resistant Electron Delocalized Molecules for Stable and Efficient Photovoltaics. *Advanced Energy Materials*, 8(13), p.1703143.

17) Zeng, Q., Zhang, X., Feng, X., Lu, S., Chen, Z., Yong, X., Redfern, S., Wei, H., Wang, H., Shen, H., Zhang, W., Zheng, W., Zhang, H., Tse, J. and Yang, B. (2018). Polymer-Passivated Inorganic Cesium Lead Halide Perovskites for High-Voltage and High-Efficiency Solar Cells. *SSRN Electronic Journal*.

18) Yang, S., Dai, J., Yu, Z., Shao, Y., Zhou, Y., Xiao, X., Zeng, X. and Huang, J. (2019). Tailoring Passivation Molecular Structures for Extremely Small Open-Circuit Voltage Loss in Perovskite Solar Cells. *Journal of the American Chemical Society*, 141(14), pp.5781-5787.

19) Buin, A., Comin, R., Xu, J., Ip, A. and Sargent, E. (2015). Halide-Dependent Electronic Structure of Organolead Perovskite Materials. *Chemistry of Materials*, 27(12), pp.4405-4412.

20) W. S. Yang et al*., Science* 356, 1376–1379 (2017)

21) Saliba, M., Matsui, T., Seo, J., Domanski, K., Correa-Baena, J., Nazeeruddin, M., Zakeeruddin, S., Tress, W., Abate, A., Hagfeldt, A. and Grätzel, M. (2016). Cesium-containing triple cation perovskite solar cells: improved stability, reproducibility and high efficiency. *Energy & Environmental Science*, 9(6), pp.1989-1997.

22) Fu, F., Pisoni, S., Jeangros, Q., Sastre-Pellicer, J., Kawecki, M., Paracchino, A., Moser, T., Werner, J., Andres, C., Duchêne, L., Fiala, P., Rawlence, M., Nicolay, S., Ballif, C., Tiwari, A. and Buecheler, S. (2019). I2 vapor-induced degradation of formamidinium lead iodide based perovskite solar cells under heat–light soaking conditions. *Energy & Environmental Science*, 12(10), pp.3074-3088.

23) Turkevych, I., Kazaoui, S., Belich, N., Grishko, A., Fateev, S., Petrov, A., Urano, T., Aramaki, S., Kosar, S., Kondo, M., Goodilin, E., Graetzel, M. and Tarasov, A. (2018). Strategic advantages of reactive polyiodide melts for scalable perovskite photovoltaics. *Nature Nanotechnology*, 14(1), pp.57-63.